



Available online at www.sciencedirect.com



Lithos 72 (2004) 117–146

LITHOS

www.elsevier.com/locate/lithos

Neogene–Quaternary magmatism and geodynamics in the Carpathian–Pannonian region: a synthesis

Ioan Seghedi^{a,*}, Hilary Downes^b, Alexandru Szakács^a, Paul R.D. Mason^c, Matthew F. Thirlwall^d, Emilian Roșu^e, Zoltán Pécskay^f, Emö Márton^g, Cristian Panaiotu^h

^a Institute of Geodynamics, 19-21, Jean-Luis Calderon Str., Bucharest 70201, Romania

^b Birkbeck/UCL Research School of Geological and Geophysical Sciences, Birkbeck College, Malet St., London WC1E 7HX, UK

^c Veining Meinesz Research School of Geodynamics, Utrecht University, Budapestlaan, 4, 3584 CD Utrecht, The Netherlands

^d Department of Geology, Royal Holloway University of London, Egham Hill, Egham, Surrey TW20 0EX, UK

^e Geological Institute of Romania, 1, Caransebeș Str., 78344 Bucharest, 32, Romania

^f Institute of Nuclear Research of the Hungarian Academy of Sciences, P.O. Box 51, Bem ter 18/c, H-4001 Debrecen, Hungary

^g ELGI, Columbus u., 17-23, 1145 Budapest, Hungary

^h Paleomagnetism Laboratory, University of Bucharest, Bălcescu 1, 70111 Bucharest, Romania

Received 29 January 2003; accepted 29 August 2003

Abstract

In the Carpathian–Pannonian region in Neogene times, westward-dipping subduction in a land-locked basin caused collision of two lithospheric blocks (Alcapa and Tisia) with the southeastern border of the European plate. Calc-alkaline and alkaline magmatism was closely related to subduction, rollback, collision and extension. From the spatial distribution of the magmatic activity, four segments can be defined: Western Segment (magmatism occurring on the Alcapa block), Central Segment (magmatism occurring on both Alcapa and the Tisia blocks), South-Eastern Segment and Interior Segment (both on the Tisia block).

Most calc-alkaline magmatism in the region resulted from melting of a heterogeneous asthenospheric mantle source modified by addition of fluids and sediment. Assimilation and fractionation processes at shallow crustal levels occurred in most of the segments, strongly masking the deeper source processes. Long-term subduction, rollback and/or delamination led to contamination of the asthenosphere beneath the Western Segment. Here, large-volume partial melts of the contaminated mantle caused underplating and crustal anatexis, leading to mixing of mantle-derived calc-alkaline magmas with crustal melts. In the Central Segment, calc-alkaline magmas were formed by subduction and rollback, followed by back-arc extension and slab breakoff. A variable mantle source is indicated in the back-arc setting and larger amount of fluid-induced metasomatism, source enrichment and assimilation nearer to the trench. In the Interior Segment, evolution from typical calc-alkaline magmas to adakite-like ones was related to extension due to fast rotations and transtensional tectonics. Here, calc-alkaline magmas formed by decompression melting of a heterogeneous crust–mantle lithosphere, while adakite-like melts resulted from fluid-dominated melting of the lithosphere. Along the South-Eastern Segment, slab breakoff was responsible for the generation of typical calc-alkaline magmas, but in the extreme south of the segment, shallow level tearing of the slab followed breakoff. Strike-slip tectonics allowed the rise of hot asthenosphere and generation of adakite-like magmas, via slab-melting, along the torn edge of the East European Plate. Alkaline basaltic volcanism with an OIB-like asthenosphere source followed the calc-alkaline stage

* Corresponding author.

E-mail address: segredi@geodin.ro (I. Seghedi).

(Western Segment), or was contemporaneous with it (South-Eastern and Interior Segments) mainly in response to local extensional tectonics.

© 2003 Elsevier B.V. All rights reserved.

Keywords: Carpathian–Pannonian region; Geodynamic processes; Calc-alkaline magmas; Adakite-like magmas; Neogene-Quaternary

1. Introduction

The Carpathian–Pannonian region of eastern central Europe is a key region for resolving the link between magmatism and tectonics (Fig. 1). Miocene–Quaternary magmatic rocks display spatial and tem-

poral geochemical variations, which may result from complex tectonic regimes: subduction, collision, post-collision and extension (Szabó et al., 1992; Csontos, 1995; Lexa and Konečny, 1998; Mason et al., 1998; Nemčok et al., 1998; Seghedi et al., 1998; Harangi, 2001). Magmatic activity developed between 20 and

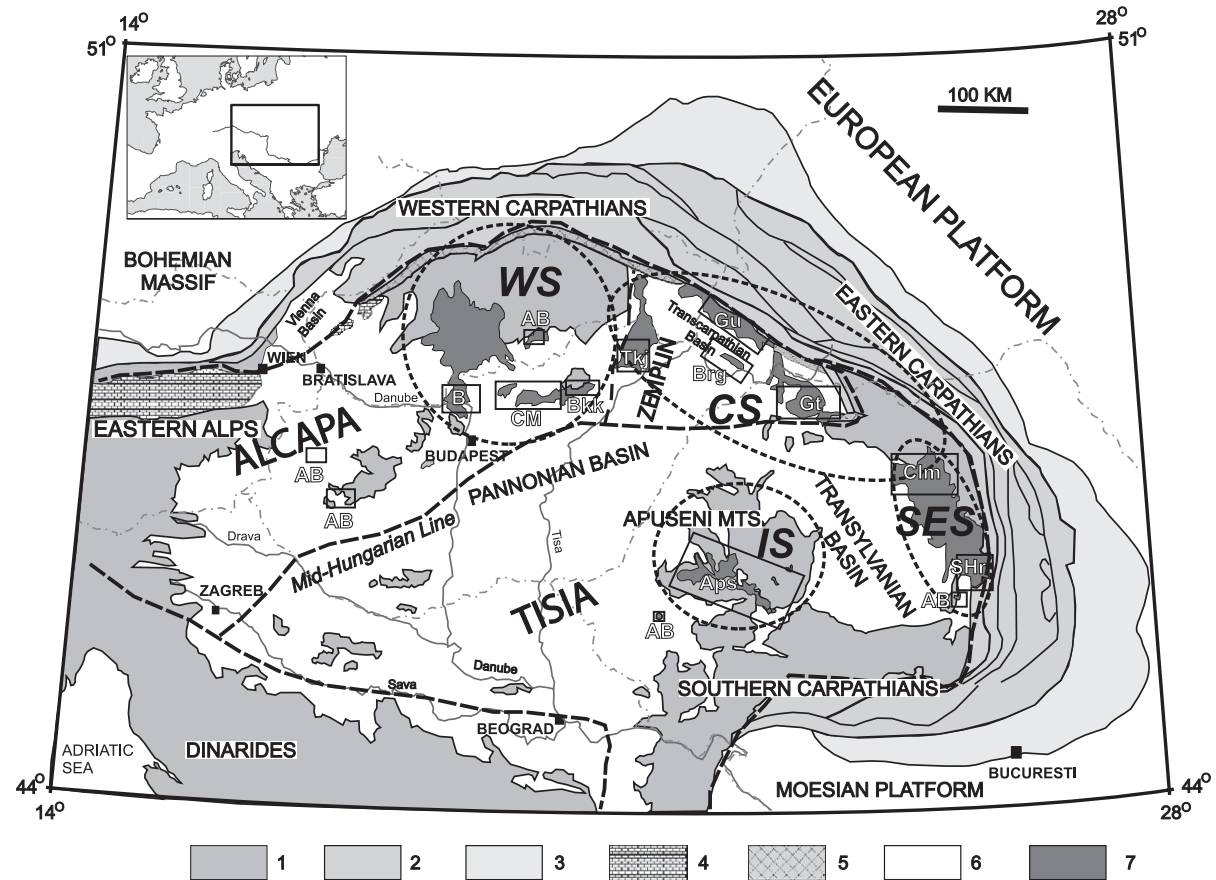


Fig. 1. Geological sketch map of Carpathian–Pannonian region showing spatial distribution of the four defined segments (WS—Western segment; CS—Central segment; SES—Southeast segment; IS—Interior segment) and location of the calc-alkaline volcanic areas (B—Börzsöny, CM—Cserhát-Mátra; Bkk—Bükk foreland; Tkj—Tokaj; Gu—Gutinski; Brg—Beregovo; Gt—Gutâi; Clm—Călimani; SHr—South Harghita; Aps—Apuseni). Alkaline basaltic areas (AB) and Intracarpathian block boundaries (ALCAPA, Zemplin, TISIA) are also shown; Legend: 1: Inner Alpine Carpathian Mountain belt and Dinarides; 2: Alpine–Carpathian Flysch belt; 3: Carpathian Molasse belt; 4: Calcareous Alps; 5: Pieniny Klippen belt; 6: Neogene–Quaternary sedimentary deposits; 7: Outcropping calc-alkaline volcanic rocks.

<0.1 Ma (Pécskay et al., 1995a) and consists of (a) large volumes of calc-alkaline magmatic products (basalts, basaltic-andesites, andesites, dacites, rhyolites) and (b) sporadic small volumes of alkaline magma types (alkalic basalts, basanites, shoshonites, lamproites).

Based on the spatial distribution, temporal evolution and geochemical features, Neogene magmatism in the Carpathian–Pannonian area can be divided into the following segments (Fig. 1): (1) a Western Segment that includes the West Carpathians and Pannonian basin (North Hungary and Central Slovakia). Here calc-alkaline volcanism occurred between ~20 and 11 Ma, with large volumes of acidic and intermediate rocks distributed randomly, sometimes transversally to the orogenic belt, and as rare small occurrences in the foreland of the Carpathians. Alkalic basaltic volcanism erupted between ~11 and 0.5 Ma, after the calc-alkaline magmatism had waned; (2) a Central Segment from Tokaj–Slanské–Vihorlat to the Călimani Mountains, where calc-alkaline acidic and intermediate volcanic activity occurred ~15–8 Ma ago. Alkalic magmatism was absent from this area; (3) a South-Eastern Segment from Călimani (north) to the Harghita Mountains (south) with dominantly intermediate calc-alkaline rocks. This magmatism was active from 10 to <1 Ma, migrating southeastward and progressively waning. Alkalic basaltic and shoshonitic volcanism was partly contemporaneous with the end of calc-alkaline volcanic activity at 1.5–0.5 Ma; (4) an Interior Segment, whose dominantly intermediate volcanic activity occurred mostly at 15–8 Ma in the Apuseni Mountain area. Alkalic basaltic and shoshonitic volcanism post-dated the calc-alkaline magmatism (2.5–1.5 Ma).

In this paper, we synthesise existing geochemical, geochronological, paleomagnetic and tectonic data from the Carpathian–Pannonian region and present new geochemical data from key areas to establish the magma sources and the processes responsible for generation of this wide variety of magmas. This study will use major, trace element and isotope data on samples belonging to representative calc-alkaline volcanic edifices, or compact volcanic areas, which evolved within distinct time intervals.

We intend to investigate the geodynamic significance of magma geochemistry in the various volcanic areas within the four segments and how this fits into

the large-scale picture of the kinematic processes in the Carpathian–Pannonian region.

2. Geodynamic setting

The Carpathians form an arcuate orogen in central and eastern Europe extending more than 1500 km between the Eastern Alps and the Balkans (Fig. 1). Its present shape originated during Tertiary times, as a result of subduction of a land-locked basin and convergence of two continental fragments with the European foreland, which acted as the lower plate (Csontos, 1995). The geometry of the region mirrors the continental margins of the pre-existing European foreland (Zweigert, 1997). Alpine Intracarpathian kinematics can be briefly summarised as follows:

- (1) Early Miocene (~24 Ma) opposite-sense translations and rotations occurred between two small continental blocks. The Alcapa block, situated north of the Mid-Hungarian lineament, underwent counterclockwise rotation (Márton and Márton, 1996; Márton, 2000), whereas the Tisia block (also known as Tisza-Dacia) (Csontos et al., 1992; Csontos, 1995) began to rotate clockwise (Pătrașcu et al., 1994; Panaiotu, 1998) (Fig. 2). The driving forces behind compression in the region have been explained as being due to: (i) extrusion of crustal blocks into free space due to continuous convergence in the Alps (Ratschbacher et al., 1991), (ii) slab pull causing roll-back along the Carpathian subduction zone (Royden, 1993), and (iii) E-directed flux of asthenosphere or relative westward drift of the lithosphere (Doglioni et al., 1999). These models explain various geological and tectonic features and have been combined in this paper in order to be consistent with the overall geodynamic evolution;
- (2) Early to Middle Miocene (24–16.5 Ma) tectonics were characterised by NE to E-ward translations of the two blocks and collision of the Alcapa block with the European continent. This generated large-scale contractions in the northern part of the Outer Carpathians (Royden, 1988; Horváth, 1993; Săndulescu, 1988) and related back-arc extension in the Pannonian Basin (Royden, 1988) (Fig. 2). The formation of Core complexes in the Pannonian

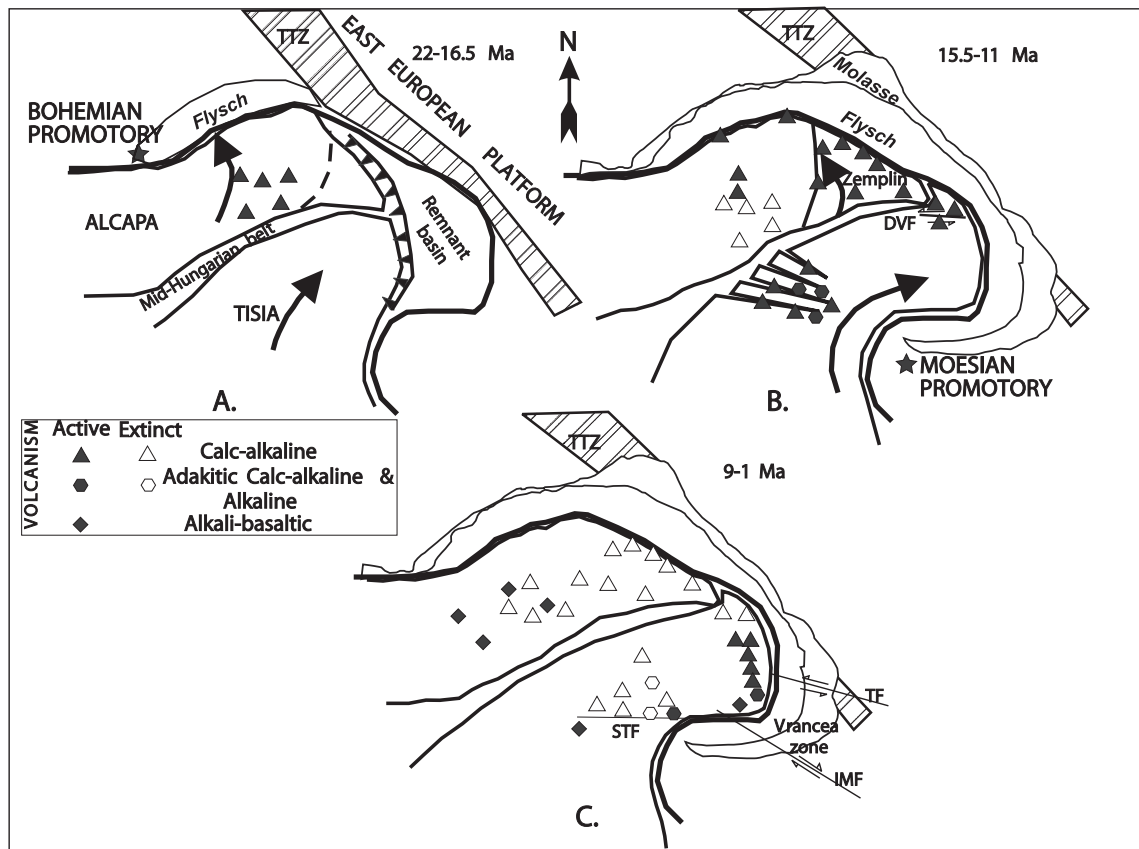


Fig. 2. Three geotectonic sketches showing a tentative model for the relationships between main structural events and evolution of magmatic activity in the Carpathian–Pannonian region, at 22–16.5, 15.5–11 and 9–1 Ma. TTZ = Tornquist–Teyssere Zone; DVF = Dragoş Vodă fault; STF = South Transylvanian fault; TF = Trotuș fault; IMF = IntraMoesian fault.

Basin and Alps is connected with this event, suggesting E–W Early Miocene (between 20 and 17 Ma) extension of the order of 200 km (Frisch et al., 2000);

- (3) During Middle Miocene (16.5–11 Ma) times, marked by a change in direction of foredeep depocenter migration (Meulenkamp et al., 1996), collision of Tisia took place and retreating subduction processes ceased due to the introduction of the East European platform in the deformation system (Małenco, 1997; Zweigert, 1997) (Fig. 2). This period coincided with very fast clockwise rotation of Tisia (around 70°), between 14.5 and 12 Ma (Panaiotu, 1999). During this period, only the northeastern part of Alcapa, known as the Zemplin Block, was subject to

continuous rigid counterclockwise block rotations from 50° to 20° (Panaiotu, 1998; Márton et al., 2000). The age of deformation of the external Carpathian nappes (accretionary wedge), which involved thrust-loading of the foreland and coincided with the end of the collision event, is Karpatian (~ 17 Ma) in the Western Segment, Badenian–Sarmatian (16.5–12 Ma) in the Central Segment and Sarmatian (13–11 Ma) in the South-Eastern Segment. This suggests an eastward progression of deformation along the thrust system (Royden et al., 1982; Csontos et al., 1992);

- (4) In the southern part of the East Carpathians, the stress field changed in Pliocene (~ 5 Ma) times from a NNE–SSW strike–slip configuration to a N–S compression, compatible with large scale

tearing and slab-breakoff in the southern part of the East Carpathians (Mason et al., 1998; Maťenco and Bertotti, 2000). In the internal zone the SSE-ward movement of the Carpathian bend area was accompanied by minor extension (Gîrbacea, 1997; Ciulavu, 1999). A flat-lying high velocity S-wave anomaly in the mantle between 400 and 650 km beneath the Carpathian–Pannonian region has been interpreted as subducted lithosphere that sank into the mantle as a result of slab detachment along strike of the Carpathian arc (Wortel and Spakman, 2000; Sperner and Lillie, 2001). Travel-time tomography also confirms the presence of a narrow slab in the Vrancea zone, which appears to be continuous down to 350 km (Wortel and Spakman, 2000).

3. Magmatic activity

Calc-alkaline magmatism in the Carpathian–Pannonian area is mostly located along the northeastern border of the Alcapa and Tisia blocks, close to the accretionary wedge of the Carpathian Flysch (Fig. 1). This includes all the Western, Central and South-Eastern Segments activity. The only exception is the Interior Segment, which is situated ~200 km away from the collision zone (Fig. 1).

There is not yet a broadly accepted view of the relationship between the volcanic activity and geotectonic evolution of the Carpathian–Pannonian region. One point of view, adopted in this paper, connects the space–time distribution of volcanism to the spatial arrangements and distribution of lithospheric blocks and postulates relationships between magmatism and subductional, collisional, post-collisional and extensional processes (Seghedi et al., 1998). The volcanic areas have been attributed to the following segments and those discussed in this study are marked with bold italics and shown in Fig. 1:

- (1) Western Segment, corresponding to the western Alcapa block, includes: Central Slovakia, Börzsöny, Cserhát-Mátra, Bükk foreland, buried volcanics in the Pannonian Basin, as well as rare magmatic occurrences in the Outer Carpathians. A slight age progression from south to north and

from west to east occurred between 20 and 10 Ma (Pécskay et al., 1995a).

- (2) Central Segment, corresponding to the Zemplín part of Alcapa block and the northern part of the Tisia block, includes the Dej tuff complex (Szakács, 2000), the Tokaj-Slanské, Vihorlat, Gutinski, Beregovo and Oaş-Gutâi volcanic areas, and the East Carpathians subvolcanic areas. The magmatic activity occurred at 15–8 Ma (Pécskay et al., 1995a,b, 2000), suggesting a very slight age migration along the arc from west to east.
- (3) South-Eastern Segment, corresponding to the central and southern Tisia block, including the East Carpathians volcanic arc (Călimani–Gurghiu–North Harghita and South Harghita volcanic areas), showing a rapid north to south along-arc migration, at 10–<1 Ma.
- (4) Interior Segment, situated within the Tisia block, with most volcanic activity developed in the Apuseni area at 15–8 Ma, cropping out mostly in the intra-mountain basins (Roşu et al., 1997, 2001) and shoshonitic volcanism in its southern part at <2 Ma.

Alkalic basaltic volcanism shows a close relationship with calc-alkaline volcanism in several areas. It was widespread in the Western Segment between 11 and 0.5 Ma (Embey-Isztin et al., 1993; Dobosi et al., 1995; Pécskay et al., 1995a,b; Harangi et al., 1995; Harangi, 2001), just as the calc-alkaline magmatism was waning. There was no alkalic basaltic volcanism within the Central Segment, but it was active southwest of South-Eastern Segment, being coeval with calc-alkaline and shoshonitic magmatism at 1.5–0.5 Ma (Seghedi et al., 1987, 2001; Downes et al., 1995b). Southwest of the Interior Segment, alkalic volcanism in the Banat area at 2.5 Ma was followed by a short episode of shoshonitic volcanism (1.5 Ma) in the Apuseni area (Pécskay et al., 1995b).

4. Geochemical evidence for petrogenetic processes

This study is based on: (a) new bulk chemical and isotopic analyses of calc-alkaline rocks (Table 1) from the Bükk, Gutâi, Tokaj areas, Dej rhyolites (Central Segment); and (b) published data from Börzsöny–Cserhát-Mátra (Western Segment) (Salters et al.,

Table 1

New bulk chemical and isotopic analyses of calc-alkaline rocks from the Bükk, Gutai, Tokaj areas and Dej rhyolites (Western and Central Segment). The data from Apuseni area (Interior Segment) have been firstly given in Roșu et al. (2001)

Sample	B-1	B-4B	B-7-1E	B-14	B-28	B-29	TD105	TD-134
Segment	WS	WS	WS	WS	WS	WS	CS	CS
Area	Bükk	Bükk	Bükk	Bükk	Bükk	Bükk	N Trans. B.	N Trans. B.
Locality	Kács	Sály	Bogács	Kisgyör	Demjén	Demjén	Măgura Ciceu	Păgălia
Age (Ma)	20	17	17	17	15	18	15	15
Rock type	Bi-Rhy	Bi-Rhy	Rhy	Rhy	Rhy	Rhy	Rhy	Rhy
SiO ₂	72.92	72.72	70.14	73.02	69.84	72.92	75.20	71.62
Al ₂ O ₃	14.42	14.55	15.65	14.44	16.65	14.62	13.29	14.62
Fe ₂ O ₃	2.15	1.85	3.11	2.29	2.52	1.75	1.56	1.99
MgO	0.78	0.72	1.05	0.47	0.89	0.57	0.45	0.78
CaO	2.25	2.33	2.73	2.23	3.08	2.37	1.62	5.99
Na ₂ O	2.64	3.13	2.69	2.77	2.55	2.95	3.64	2.73
K ₂ O	4.236	4.088	4.088	4.186	4.015	4.201	3.665	1.46
TiO ₂	0.19	0.196	0.349	0.187	0.272	0.2	0.161	0.32
MnO	0.037	0.041	0.039	0.03	0.04	0.035	0.02	0.08
P ₂ O ₅	0.071	0.076	0.097	0.079	0.093	0.093	0.086	0.1
Total	99.92	99.93	100.2	99.91	100.18	99.94	99.89	99.69
Mg#	0.419	0.438	0.401	0.289	0.413	0.393	0.364	0.437
LOI	3.04	2.39	2.92	2.87	3.31	2.28	2.73	6.94
Ni	4.8	4.7	7	5.2	5	4.7	10.6	8.9
Cr	9.8	9.7	15.6	6	11	10.8	21.4	13.6
V	23.4	21.6	38.1	20.7	36.1	22.6	11.3	22.1
Sc	4.9	4.6	13.1	4.7	6.2	5.2	6.4	10.4
Cu	0.9	1.4	4.5	2.6	7.4	0.5	1.3	1.9
Zn	36.1	36.9	53.3	37.7	45.5	34.9	24.1	27.7
Ga	15.3	15.5	17.9	15.3	15.7	15.6	16.1	16.1
Pb	27.1	27.8	25.9	29	28.2	28.1	18.2	7.4
Sr	187.2	195.4	201.5	180.5	242.9	203.9	128.2	619.9
Rb	142.6	145.9	142.7	150	169.6	146.9	77.9	58.4
Ba	807	853.3	900.2	783.5	741.1	865.2	902.4	734.5
Zr	114.8	112.3	228.5	112.9	151.2	120.4	137.8	224.1
Nb	11.6	11.5	14.6	11.6	10.4	11.4	13.6	11.8
Th	20.3	21.3	19.4	20.9	23.1	20.8	12.7	7
Y	19.3	19.5	33.9	21.4	17.6	19.8	23	21.6
La	37.8	38.1	52	35.1	32.4	37.3	33.8	31.6
Ce	63.8	66.3	101	62.4	49.9	64.9	61.2	56.8
Nd	23.3	23	40.6	23.2	16.9	23.8	24.9	22.6
⁸⁷ Sr/ ⁸⁶ Sr	—	0.710327	0.711368	0.710370	0.707728	0.710307	0.708810	0.708852
¹⁴³ Nd/ ¹⁴⁴ Nd	—	0.512252	0.512220	—	0.512433	—	0.512418	0.512439
$\delta^{18}\text{O}$	—	—	—	—	—	—	—	—
La	—	40.2	55.6	37.6	—	41.4	34.8	28.9
Ce	—	75.87	112.06	70.83	—	77.67	70.39	56.96
Pr	—	7.7	12.3	7.37	—	8.01	7.65	6.3
Nd	—	24.1	42.3	23.5	—	25.1	26.2	21
Sm	—	3.68	7.02	3.82	—	3.82	4.72	3.49
Eu	—	0.83	1.36	0.83	—	0.89	0.83	1.15
Gd	—	3	5.97	3.2	—	3.12	4.34	3.43
Dy	—	2.85	5.5	3.11	—	2.94	3.92	3.45
Ho	—	0.55	1.08	0.62	—	0.58	0.75	0.68
Er	—	1.54	2.84	1.73	—	1.59	2.01	1.97
Yb	—	1.76	2.8	1.96	—	1.79	2.05	2.03
Lu	—	0.29	0.44	0.32	—	0.29	0.32	0.33

Table 1 (continued)

Sample	TD-145-1A	TD-145-4A	SKH-23	SKH-25	2G	3G	4G
Segment	CS	CS	CS	CS	CS	CS	CS
Area	N Trans. B.	N Trans. B.	Tokaj M.	Tokaj M.	Gutái M.	Gutái M.	Gutái M.
Locality	Šoimeni	Šoimeni	Kopasz	Patkobánya	Izvoare Qua.	Firiza Qua.	Firiza V.
Age (Ma)	15	15	11.7	12.0	10.8	10.1	10.7
Rock type	Rhy	Rhy	Px And	Dac	Px Bas-And	Px Dac	Px Am And
SiO ₂	73.56	77.80	58.09	64.39	54.83	64.01	61.34
Al ₂ O ₃	13.27	12.47	17.30	15.93	18.94	16.56	15.39
Fe ₂ O ₃	1.55	0.97	7.69	5.23	8.02	5.45	6.23
MgO	0.81	0.65	2.99	2.01	3.91	2.02	3.37
CaO	5.09	3.38	6.50	4.18	8.11	5.47	6.49
Na ₂ O	2.83	2.56	3.15	3.59	3.04	3.20	2.95
K ₂ O	2.26	1.61	2.362	3.267	1.607	2.178	2.921
TiO ₂	0.22	0.15	1.131	0.76	0.881	0.6	0.667
MnO	0.03	0.01	0.148	0.091	0.156	0.072	0.138
P ₂ O ₅	0.09	0.08	0.333	0.244	0.194	0.146	0.212
Total	99.71	99.68	99.95	99.88	99.85	99.84	99.86
Mg#	0.508	0.572	0.435	0.432	0.491	0.423	0.517
LOI	7.23	5.14	1.68	0.81	1.13	1.93	0.72
Ni	8.4	12.7	7.3	6.9	7.7	4	5.5
Cr	18.6	26.1	25	16.9	8.8	6.6	24
V	12.5	9.3	135.3	81.2	192.9	105.9	179
Sc	7.3	4.7	24.4	14.3	24.1	21.7	24.9
Cu	0.7	0.5	18.5	10.7	26.7	8.5	15
Zn	16	12.5	79	60.7	72.9	56.5	66.3
Ga	14.8	13	19.9	18.9	19	17.2	16.8
Pb	8.9	8.9	12.5	17.8	7.7	9	12.9
Sr	422.2	404.9	301.9	233	260.8	218.4	243.1
Rb	87.8	54.9	88.4	121.7	44.3	71.8	64
Ba	724.1	864.2	392.6	530.8	329.5	408.9	391.7
Zr	162.3	134.8	192.3	221.8	118.1	127.6	116.1
Nb	12.5	10.7	14.6	19.8	8.3	8.1	8.1
Th	10.2	7.1	8.4	16.1	4.8	7	6.4
Y	17.8	42.3	32.1	29.4	32.2	25.9	24
La	33.2	25.8	27.6	37.9	17.5	20.2	19.3
Ce	61	47.4	58	69.4	41.4	39.2	35.9
Nd	24.4	17.7	27	28.2	22.3	18.2	17.5
⁸⁷ Sr/ ⁸⁶ Sr	0.709104	0.708932	—	0.707424	0.708330	0.708940	0.710296
¹⁴³ Nd/ ¹⁴⁴ Nd	—	—	—	0.512432	0.512387	—	0.512409
$\delta^{18}\text{O}_{\text{px}}$	—	—	—	6.97	6.61	—	—
La	32.9	25.9	—	36	17.2	18.7	18.4
Ce	65.58	53.3	—	70.69	40.64	39.78	38.25
Pr	7.04	5.61	—	7.95	5.08	4.6	4.43
Nd	23.7	18.6	—	28.1	21.4	17.5	17.4
Sm	3.87	3.04	—	5.15	4.71	3.59	3.5
Eu	0.94	1.01	—	1.11	1.25	0.97	0.97
Gd	3.27	3.0	—	5.07	5.17	3.86	3.7
Dy	2.96	4.82	—	4.82	5.33	3.99	3.89
Ho	0.56	1.19	—	0.95	1.07	0.8	0.78
Er	1.47	4.19	—	2.66	3.0	2.28	2.22
Yb	1.53	5.32	—	2.65	2.86	2.31	2.26
Lu	0.24	0.89	—	0.43	0.45	0.38	0.37

(continued on next page)

Table 1 (continued)

Sample	5G	6G	7G	8G1	9G	363 ^a
Segment	CS	CS	CS	CS	CS	IS
Area	Gutâi M.	Gutâi M.	Oaş-Gutâi M.	Gutâi M.	Gutâi M.	Apuseni M.
Locality	Blidari Qua.	V. Romana Qua.	Oraşul Nou	Laleaua Albă	Serp. Gutâi	Baia de Arieş
Age (Ma)	10.3	10.7	11.0	9.3	10.5	8.6
Rock type	Px And	Px And	Rhy	Px Am Bi And	Px Bas-And	Am Bi Q And
SiO ₂	56.82	59.89	76.09	59.47	55.35	61.70
Al ₂ O ₃	19.37	17.17	13.57	16.86	18.72	16.55
Fe ₂ O ₃	7.74	6.98	0.88	6.93	8.06	5.62
MgO	2.95	3.39	0.21	3.40	3.80	2.93
CaO	7.66	6.68	1.25	6.74	8.18	5.87
Na ₂ O	2.75	2.70	3.15	3.42	2.44	3.29
K ₂ O	1.477	1.91	4.30	1.91	1.868	1.99
TiO ₂	0.838	0.717	0.141	0.691	0.884	0.67
MnO	0.143	0.128	0.01	0.145	0.176	0.14
P ₂ O ₅	0.189	0.136	0.101	0.137	0.234	0.28
Total	100.09	99.85	99.84	99.95	99.89	99.04
Mg#	0.430	0.490	0.321	0.493	0.483	0.508
LOI	1.12	1.46	1.07	1.64	1.17	0.36
Ni	5.8	5.4	3.5	16.3	6.5	7.3
Cr	11.3	11.2	3.9	46.5	11.2	25.3
V	175.9	164.7	7.5	148.3	217.3	150
Sc	26.1	26.4	4.3	19.9	28.5	20.4
Cu	16.8	11.5	1	28.1	32.4	31.8
Zn	72	68.8	20.6	62.9	91.9	64.3
Ga	18.9	18.7	14.6	17.1	19.1	17.8
Pb	11.5	9.6	18.1	19.7	8.4	19.7
Sr	288.4	230.5	109.2	361.4	264.7	665
Rb	49.7	62.3	159.2	100.2	47.9	60
Ba	334.9	369.5	619.4	847.3	302.2	1211
Zr	131.7	121.6	145.2	143.4	119.1	156
Nb	7.5	8.4	9.9	13.2	8.7	17.4
Th	4.6	6.5	12.3	14.8	4.3	8.8
Y	23.1	24.3	28.5	22.8	33.5	21.2
La	15.9	19.3	29.9	28.6	19.1	29.7
Ce	34	39.6	52.8	54.9	39.1	57
Nd	17.4	18.8	22.2	23.3	22.2	25
⁸⁷ Sr/ ⁸⁶ Sr	—	0.709200	0.708280	—	—	0.704704
¹⁴³ Nd/ ¹⁴⁴ Nd	—	0.512365	0.512467	—	—	0.512667
$\delta^{18}\text{O}$	—	—	—	—	—	—
La	18.5	—	26.3	—	—	30.6
Ce	39.92	—	54.54	—	—	62.59
Pr	4.63	—	6.15	—	—	7.34
Nd	17.9	—	21.4	—	—	21
Sm	3.56	—	4.05	—	—	4.62
Eu	0.99	—	0.7	—	—	1.27
Gd	3.77	—	3.9	—	—	3.95
Dy	3.88	—	4.22	—	—	3.42
Ho	0.79	—	0.86	—	—	0.67
Er	2.24	—	2.48	—	—	2.06
Yb	2.24	—	2.76	—	—	1.9
Lu	0.36	—	0.45	—	—	0.32

Table 1 (continued)

Sample	394 ^a	400 ^a	401 ^a	767 ^a	776 ^a	788 ^a
Segment	IS	IS	IS	IS	IS	IS
Area	Apuseni M.					
Locality	Sacarâmb	Nucet Hill	Brad	Cetraş V.	Zâmbriţa	Detunata
Age (Ma)	11.2	12.6	11.4	11.7	10.5	7.4
Rock type	Am Bi Q And	Am Bi And	Am Bi And	Am Bi Q And	Am Bi ThrAnd	Px Bas-And
SiO ₂	62.33	58.94	63.58	61.41	58.09	55.20
Al ₂ O ₃	16.97	19.18	17.93	17.49	15.79	16.00
Fe ₂ O ₃	5.2	5.51	4.53	5.23	5.82	6.83
MgO	3.32	2.76	1.50	3.69	4.85	6.36
CaO	5.95	6.76	5.43	7.05	6.93	9.71
Na ₂ O	3.27	3.87	3.49	3.51	3.74	2.84
K ₂ O	1.88	1.88	1.89	1.47	2.92	1.45
TiO ₂	0.53	0.52	0.53	0.56	0.71	0.90
MnO	0.13	0.11	0.24	0.12	0.1	0.15
P ₂ O ₅	0.20	0.21	0.18	0.18	0.34	0.26
Total	99.78	99.74	99.3	100.71	99.29	99.70
Mg#	0.558	0.498	0.397	0.583	0.623	0.649
LOI	1.62	0.43	1.04	0.80	0.57	0.26
Ni	14.3	4.2	5.8	22	56	26.1
Cr	83.5	11.9	12.8	83.4	89.9	224
V	133	190	106	131	149	205
Sc	20	19	15.6	17.7	18.8	38.4
Cu	29.1	30.2	14.1	33.4	25.3	61.3
Zn	55.8	47.2	67.9	60.6	65.8	59.1
Ga	17	17.8	17.5	17.8	19.7	23.4
Pb	17	30	10.8	21.9	51.1	11.6
Sr	635	1742	321	1005	2770	596
Rb	54.6	37.3	62.6	39.5	53.7	40.6
Ba	1274	1897	455	945	2165	568
Zr	95.5	70.1	106	101	171	108
Nb	10.3	7.9	8.1	9	16.3	16.8
Th	7.5	11.7	5.3	5.7	21.6	4.6
Y	19.6	17.8	29.3	19.6	22.2	19.1
La	25.5	48.8	24.9	25	92.7	20.5
Ce	45.8	84.2	38.6	43	169.8	40
Nd	19.9	30.2	22.5	20.1	67.2	19.2
⁸⁷ Sr/ ⁸⁶ Sr	0.704744	0.703982	0.705608	0.704502	0.704250	0.704400
¹⁴³ Nd/ ¹⁴⁴ Nd	0.512656	0.512678	0.512593	0.512634	0.512609	0.512689
$\delta^{18}\text{O}_{\text{am}}$	—	—	—	5.93	5.30	—
La	25.2	46.5	23.3	23.4	91.7	20.4
Ce	47.37	85.2	41.14	45.76	178.77	42.97
Pr	5.58	9.17	6.02	5.46	20.44	5.06
Nd	15.4	27.5	21.7	19.1	66.4	19.4
Sm	3.33	4.2	4.16	3.29	9.43	3.76
Eu	1.02	1.21	1.25	1.05	2.51	1.22
Gd	3.05	3.3	4.66	3.4	6.5	3.79
Dy	2.8	2.65	4.41	2.99	4.02	3.4
Ho	0.56	0.55	0.88	0.59	0.75	0.66
Er	1.78	1.57	2.57	1.66	1.56	1.88
Yb	1.66	1.57	2.48	1.71	1.64	1.73
Lu	0.28	0.26	0.39	0.27	0.25	0.27

(continued on next page)

Table 1 (continued)

Sample	790 ^a	2479 ^a	5199 ^a	6922 ^a	UR-3 ^a
Segment	IS	IS	IS	IS	IS
Area	Apuseni M.	N Apuseni M.	Apuseni M.	Apuseni M.	Apuseni M.
Locality	Bucium	Moigrad	Chișindia	Zlatna	Uroiu Hill
Age	14.6	12.4	12.8	12.6	1.6
Rock type	Am Px And	Am Px Bas-And	Px And	Am Px Md	Am Bi Thr-And
SiO ₂	61.43	56.51	60.56	60.67	61.18
Al ₂ O ₃	18.63	18.30	16.91	17.72	15.64
Fe ₂ O ₃	6.05	7.62	7.14	7.19	4.04
MgO	2.45	3.18	3.19	2.54	2.96
CaO	7.06	7.56	7.09	6.73	4.79
Na ₂ O	2.88	3.44	3.19	3.38	4.21
K ₂ O	1.39	1.15	1.30	1.49	5.32
TiO ₂	0.64	0.87	0.71	0.63	0.87
MnO	0.13	0.12	0.11	0.18	0.07
P ₂ O ₅	0.14	0.29	0.18	0.14	0.61
Total	100.8	99.04	100.38	100.67	99.69
Mg#	0.445	0.453	0.469	0.412	0.592
LOI	0.95	0.80	0.44	1.25	0.23
Ni	3.9	4.9	14.5	6.2	41
Cr	15.9	11.8	24.8	9.8	38.5
V	140	146	176	146	84.3
Sc	20.2	19.2	23.9	18.4	7
Cu	11.5	8.9	57.3	70.8	20.4
Zn	59.8	35.5	61.2	54.8	61.3
Ga	17.4	18.9	16.4	17.2	23.4
Pb	7.7	2.5	6.6	34.3	37.1
Sr	212	557	249	391	2353
Rb	50.1	34.6	44.2	45.6	58.6
Ba	262	181	199	386	1878
Zr	101	130	118	88.9	317
Nb	7.8	6.9	6.3	7	24.9
Th	4.6	3.2	4.5	3	20.1
Y	22.8	24	28.5	20.3	16.5
La	16.3	20.1	14.4	12	106
Ce	34.4	42	26.3	27.2	184
Nd	16.8	20.7	15.1	13	63
⁸⁷ Sr/ ⁸⁶ Sr	0.708312	0.705713	0.704640	0.706252	0.704441
¹⁴³ Nd/ ¹⁴⁴ Nd	0.512421	0.512580	0.512778	0.512426	0.512680
$\delta^{18}\text{O}$	—	—	—	—	—
La	15.7	20.7	11.5	13.9	111.3
Ce	35.12	45.47	27.79	30.57	205.7
Pr	4.1	5.27	3.56	3.57	21.5
Nd	15.8	20.7	14.6	13.8	67.3
Sm	3.28	3.98	3.38	2.94	8.76
Eu	0.97	1.28	0.94	0.87	2.32
Gd	3.48	4.0	4.13	3.23	5.53
Dy	3.68	3.85	4.59	3.32	3.26
Ho	0.73	0.76	0.93	0.65	0.57
Er	2.15	2.18	2.87	1.91	1.05
Yb	2.13	2.11	2.74	1.75	1.02
Lu	0.32	0.32	0.43	0.26	0.15

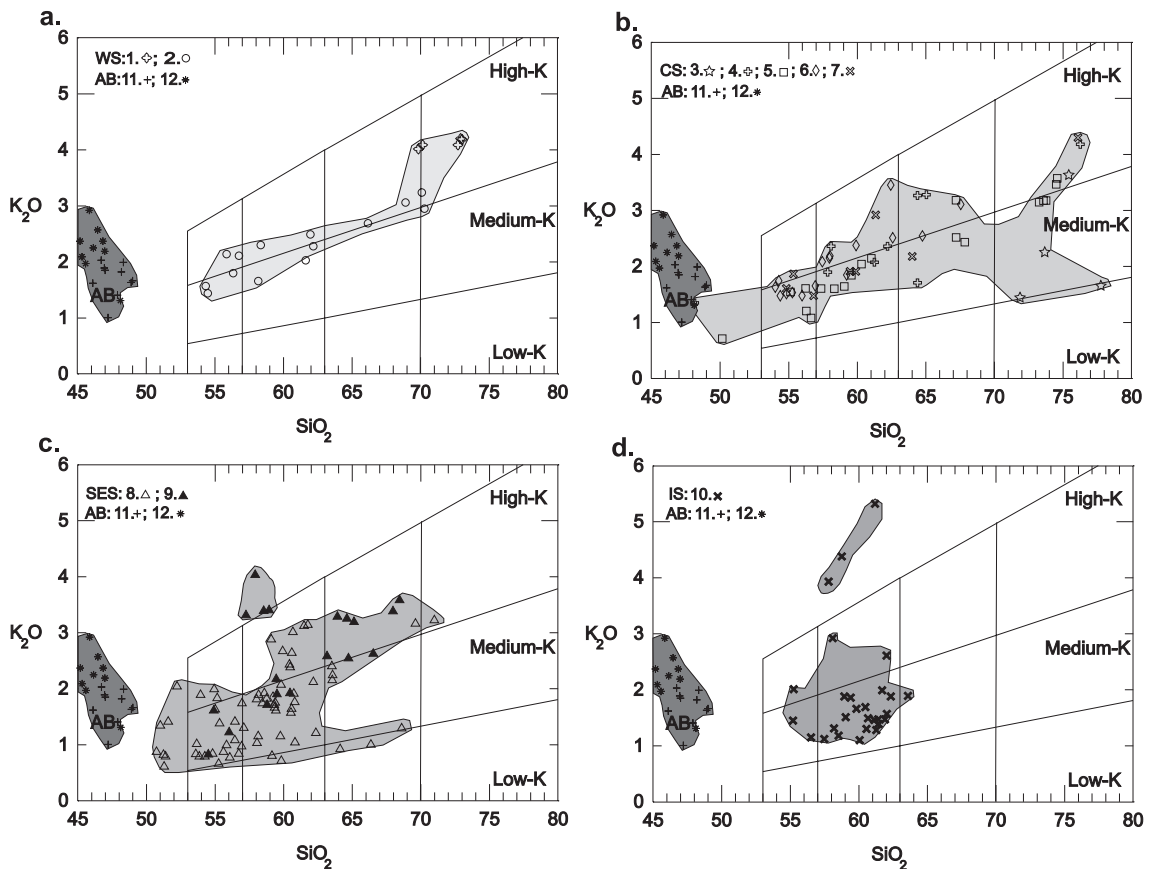


Fig. 3. SiO_2 vs. K_2O for Carpathian–Pannonian region volcanic rocks; Symbols: Western Segment (WS): 1—Bükk rhyolites; 2—Börzsöny, Cserhát–Mátra; Central Segment (CS): 3—Dej rhyolites; 4—Tokaj; 5—Beregovo; 6—Gutinski; 7—Gutái; South-Eastern Segment (SES): 8—Călimani; 9—South Harghita; Interior Segment (IS): 10—Apuseni; Alkalic basalts (AB): 11—Perşani and Banat alkalic basalts; 12—Little Hungarian Plain, Balaton and Nógrád—Novohrad alkalic basalts. Data from Salters et al. (1988), Embey-Isztin et al. (1993), Dobosi et al. (1995), Downes et al. (1995a,b), Harangi et al. (1995, 2001), Mason et al. (1996), Seghedi et al. (2001), Roșu et al. (2001) and this work. Field of Western Segment filled with 10% black; field of Central Segment filled with 20% black; field of South-Eastern Segment filled with 30% black; field for Interior Segment filled with 40% black and field of Alkalic basalts filled with 50% black.

1988; Downes et al., 1995b; Harangi et al., 2001), Ukrainian volcanic areas and Tokaj areas (Central Segment) (Salters et al., 1988; Downes et al., 1995b; Seghedi et al., 2001), Călimani volcanic edifice (South-Eastern-N Segment) and South Harghita (South-Eastern-S Segment) (Mason et al., 1996).

Most of these data were obtained in the same XRF and isotope laboratories (Royal Holloway, University of London), ensuring excellent analytical comparability and reliability. Analytical techniques have been presented in previous publications (e.g. Downes et al., 1995a,b; Mason et al., 1996; Seghedi et al., 2001).

Notes to Table 1:

Major and trace element data were determined by XRF analysis and calculated on a volatile-free basis. Major elements are given in wt.% and trace elements in ppm. For isotope analyses ϵ_{Nd} is reported relative to CHUR value of 0.51264. Errors quoted are the internal precision at 2 S.E. for Sr and Nd isotope analyses. Average for the Sr standard SRM 987 is 0.710239 ± 10 and for Nd Aldrich standard is 0.511414 ± 4 . Abbreviations: WS, CS, IS—Western, Central, and Interior Segments; bas-and=basaltic-andesite and=andesite, dac=dacite, rhy=rhyolite, thr=thrahy-andesite, Md-micro-diorite, Px=pyroxene, Am=amphibole, Bi=biotite, Q=quartz.

^a Data from Roșu et al. (2001).

Many subduction-related volcanic suites display geochemical and isotopic evidence for involvement of a crustal component (e.g. Hawkesworth et al., 1977; James, 1981; James and Murcia, 1984; Ellam and Harmon, 1990; Smith et al., 1996; Mason et al., 1996). Three possible contamination mechanisms have been invoked: (1) source contamination by addition of subduction components derived from the descending slab and its associated sediments (e.g. Pearce, 1982), (2) crustal contamination acquired via assimilation-fractional crystallisation within crustal magma chambers (James, 1981; Davidson et al., 1990), and (3) mixing between a mantle-derived magma and a crustal-derived melts (e.g. Harangi et al., 2001). The discussion will primarily focus on combined crustal assimilation-fractional crystallisation (AFC) source contamination (SC) and mixing

effects, which must be quantified and separated before an attempt can be made to constrain the magmatic sources (e.g. mantle, slab-derived melts, crust) and to distinguish between different mantle sources (asthenospheric, lithospheric) and crustal sources.

4.1. Major, trace element and radiogenic isotope data

Major, trace element and isotope characteristics of the calc-alkaline magmatic rocks from the Carpathian–Pannonian area have long been recognised as being typical for subduction-related magmas (e.g. Salters et al., 1988; Szabó et al., 1992; Downes et al., 1995a,b; Seghedi et al., 1995; Mason et al., 1995, 1996; Lexa and Konečny, 1998; Kovacs, 2002). According to the K_2O – SiO_2 diagram (Fig. 3), the magmatic rocks are mostly basaltic–andesites and

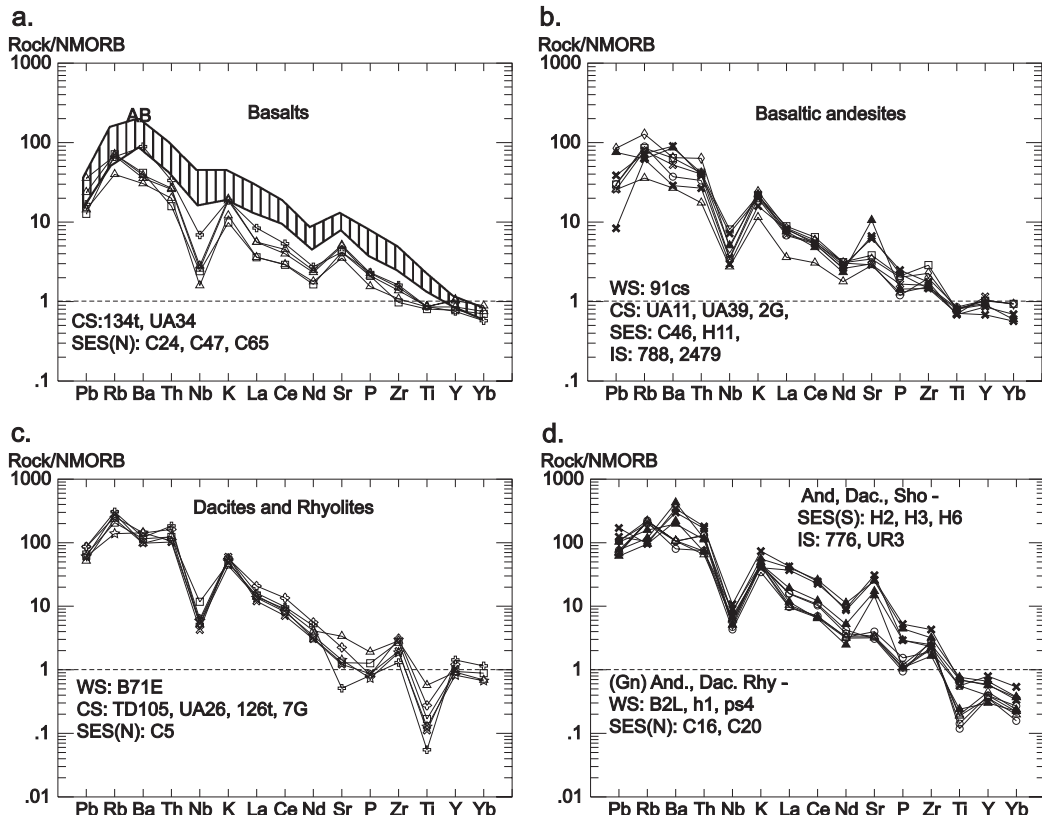


Fig. 4. N-MORB normalized incompatible trace element diagrams for selected representative basalts (a), basaltic andesites (b), dacites and rhyolites (c) and some unusual andesites, dacites and shoshonites (d), using the normalizing coefficient of Sun and McDonough (1989); Abbreviations: WS, CS, SES–N, SES–S, IS—Western, Central, South-Eastern-north, South-Eastern-south and Interior Segments; Gn—garnet, and—andesite, dac—dacite, rhy—rhyolite. Symbols and data as in Fig. 3.

andesites, but basalts, dacites and rhyolites are also present. Samples from each separated segment generally plot in a common area between the medium- and high-K fields. A few shoshonites are present in the Interior and South-Eastern-S Segments. Low-K andesites and dacites occur only in Călimani (South-Eastern-N Segment). Bükk rhyolites (Western Segment) plot in the high-K field as do rhyolites from Gutâi and Tokaj and some from Beregovo (Central Segment). Only the Dej rhyolites (Central Segment) are scattered in the medium-K field.

Incompatible element abundances in a representative selection of Carpathian–Pannonian calc-alkaline basalts and basaltic andesites are normalised to N-MORB (Fig. 4). Basalts from Beregovo, Tokaj (Central Segment), but mostly Călimani (South-Eastern-N

Segment) are variably enriched in large ion lithophile elements (LILE) and light rare earth elements (LREE) and also show variable depletion of Nb, a characteristic feature for subduction-related magmas. Basaltic andesites from Western, Central and South-Eastern Segments show patterns similar to those of the basalts. Similar features in basalts and basaltic andesites throughout the Carpathian–Pannonian region suggest that such geochemical characteristics are typical of derivation from subduction-modified mantle on a regional scale. Exceptions are basaltic-andesites from Interior and South-Eastern-S Segments, which show an unusually large range, higher LILE and Sr contents (Fig. 4b). Similar typical behaviour also occurs in dacites and rhyolites from Western, Central and South-Eastern Segments (Fig. 4c). In contrast, a

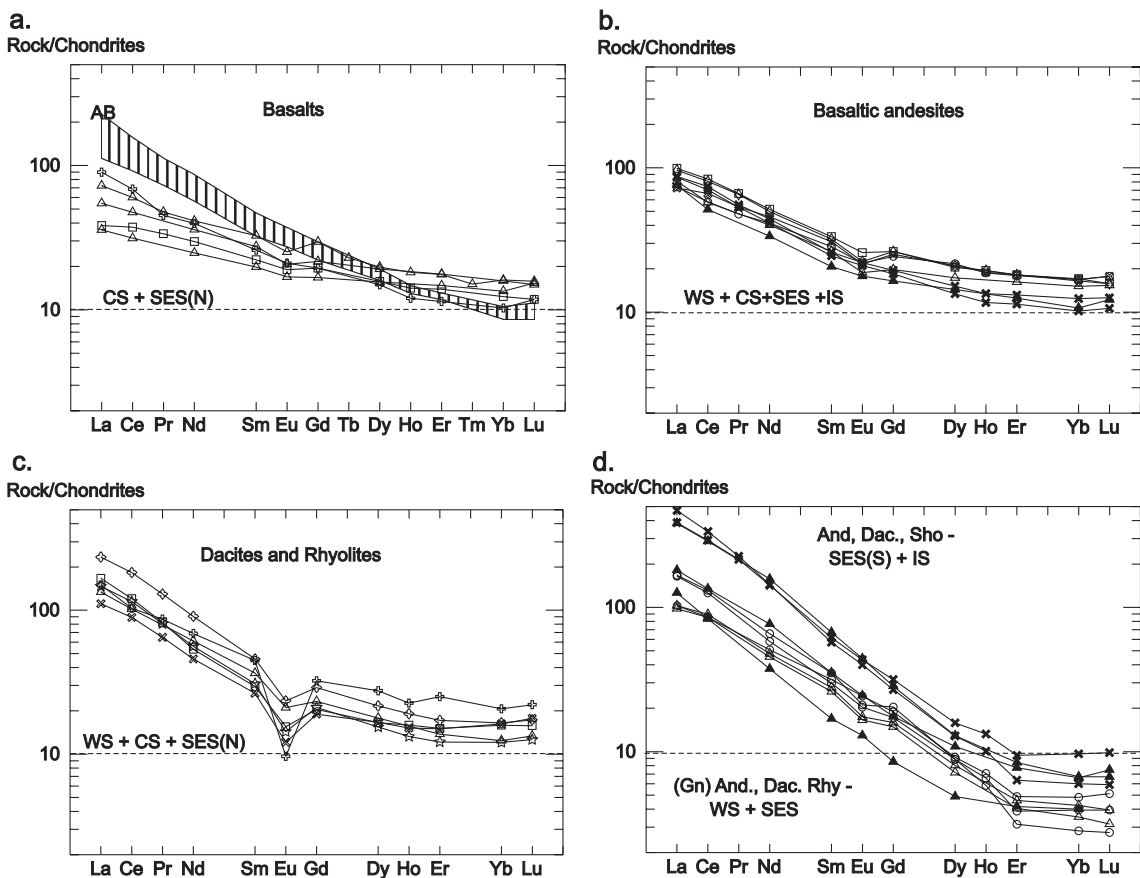


Fig. 5. Chondrite-normalized rare earth element diagram for selected representative basalts (a), basaltic andesites (b), dacites and rhyolites (c) and some unusual andesites, dacites and shoshonites (d). Normalizing coefficients from Sun and McDonough (1989). Symbols and data as in Fig. 3. Abbreviation as in Fig. 4.

distinct trend can be seen for andesites and dacites from Interior and South-Eastern-S Segments, which show the same high Ba, LREE and Zr and low heavy rare earth elements (HREE) abundance as basaltic andesites (Fig. 4d). HREE depletion is characteristic also for garnet-bearing andesites, dacites and rhyolites from Western and South-Eastern-N Segment (Fig. 4d).

REE patterns for the same representative rocks from Western, Central and South-Eastern Segments (Fig. 5) show an overall increase in total REE content (particularly LREE) and a larger Eu anomaly with increasing SiO₂. Andesites, dacites and shoshonites of Interior and South-Eastern-S Segments behave differently, showing LREE increase along with HREE decrease, but without any Eu anomaly. Garnet-bearing andesites, dacites and rhyolites from Western and South-Eastern-N Segments show similar patterns to those of Interior and South-Eastern-S Segments andesites dacites and shoshonites, with occasionally a slight Eu anomaly and higher HREE depletion (Fig. 5).

The $^{86}\text{Sr}/^{87}\text{Sr}$ vs. $^{143}\text{Nd}/^{144}\text{Nd}$ diagram reveal a large isotopic variation (Fig. 6). Some samples reach strongly enriched compositions overlapping the local Upper Crust field (Mason et al., 1996). The four segments are largely discriminated by their Sr–Nd isotopic ratios, with magmas from South-Eastern and

Interior Segments showing the lower $^{86}\text{Sr}/^{87}\text{Sr}$ and higher $^{143}\text{Nd}/^{144}\text{Nd}$ compared with those from Western and Central Segments.

4.2. Fractional crystallisation and crustal assimilation

Interaction between magma and crustal rocks may occur during ascent and storage in magma chambers, where fractional crystallisation, assimilation and mixing can take place before the magmas reach the surface. These processes can modify the major, trace element and isotopic compositions of magmas and their effect need to be filtered out prior to discussion of source processes.

Correlation of $^{87}\text{Sr}/^{86}\text{Sr}$ with SiO₂ provides evidence for the occurrence of all contamination mechanisms in the volcanic suites of the Carpathian–Pannonian region (Fig. 7). For several individual areas the transition from basalts or basaltic andesites to dacites or rhyolites occurs over a generally narrow range of $^{87}\text{Sr}/^{86}\text{Sr}$ (Mason et al., 1996; Seghedi et al., 2001), even though the whole $^{87}\text{Sr}/^{86}\text{Sr}$ variation is much larger. The lowest and highest SiO₂ values of each trend suggest that fractional crystallisation (FC) or assimilation-fractional crystallisation processes

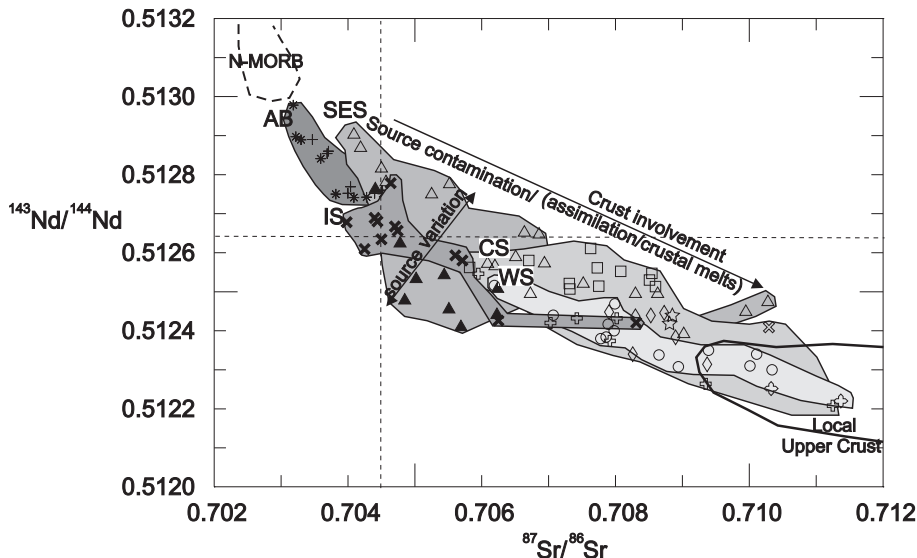


Fig. 6. $^{87}\text{Sr}/^{86}\text{Sr}$ vs. $^{143}\text{Nd}/^{144}\text{Nd}$ variation, suggesting implication of source contamination, crustal involvement via crustal assimilation or mixing with crustal melts and source variation of Carpathian–Pannonian volcanic rocks. Symbols, data and fields as in Fig. 3. Field of East Carpathian upper crust from Mason et al. (1996).

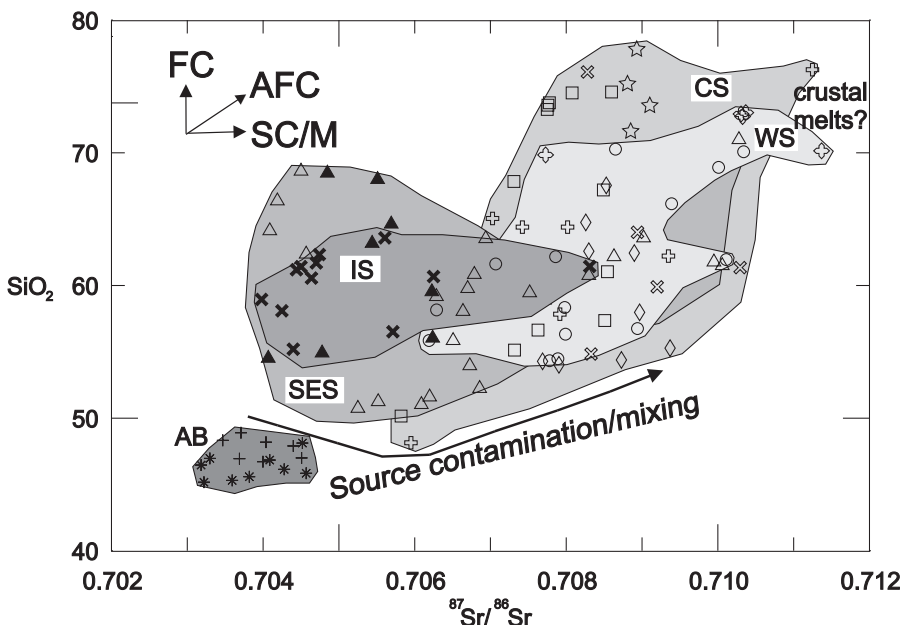


Fig. 7. SiO_2 vs. $^{87}\text{Sr}/^{86}\text{Sr}$ diagram of Carpathian–Pannonian volcanic rocks, suggesting possible contamination mechanisms. Symbols, data and fields as in Fig. 3.

(AFC) developed mostly in upper crustal magma chambers. The fractionating mineral assemblage (i.e. plagioclase, olivine and pyroxenes) caused the increase in SiO_2 , whereas the shift toward higher $^{87}\text{Sr}/^{86}\text{Sr}$ may be related to assimilation processes particularly in the case of magmas from the Western, Central Segment and South-Eastern-N Segments (Fig. 7). However, mixing between mantle-derived magmas and crustal material may be an alternative solution for certain Western and Central Segment magmas (e.g. Harangi et al., 2001). Magmas from the South-Eastern-S and Interior SegmentS do not satisfy the criteria for significant fractionation and assimilation processes, since they show a narrow SiO_2 interval and lower $^{87}\text{Sr}/^{86}\text{Sr}$ ratios.

The distinction between source contamination and crustal assimilation can be more easily recognised using Sr–O isotopic modelling (James, 1981; Ellam and Harmon, 1990). Oxygen isotope enrichment is a sensitive indicator of crustal contamination, while Sr isotopes can be either sensitive or insensitive to it (Ellam and Harmon, 1990; Davidson et al., 1990; Mason et al., 1996). $\delta^{18}\text{O}$ data are available on mineral separates (mainly pyroxenes, amphiboles) from Western, Central and South-Eastern Segments locations

(Downes et al., 1995b; Mason et al., 1996; Dobosi et al., 1998; Seghedi et al., 2001) and new data from Gutâi, Apuseni and Tokaj are given in Table 1. Fig. 8 shows plots of $\delta^{18}\text{O}$ in mafic minerals vs. $^{87}\text{Sr}/^{86}\text{Sr}$ in Carpathian–Pannonian magmas. High and variable $\delta^{18}\text{O}$ for volcanic rocks of the Carpathians may reflect either assimilation of continental crust or source characteristics, or a combination of these two processes. This can be tested using modelling.

Assimilation-fractional crystallisation curves (AFC) can be modelled using the most isotopically primitive compositions which belong to South-Eastern Segment–N (sample C65) and Central Segment (sample 134t) and a crustal assimilant (average value for East Carpathians local crust from Mason et al., 1996). That large $\delta^{18}\text{O}$ variations can be accounted for by AFC processes is clearly shown by the steep O–Sr arrays of Fig. 8, starting from a primary magma close to the most “primitive” samples. AFC probably produced intermediate to acid magmas of Western, Central and South-Eastern-N Segments, with less contaminated magmas occurring in the Beregovo area (Central Segment). Between 5% and 20% upper crustal contaminant is required in the AFC modelling in these areas.

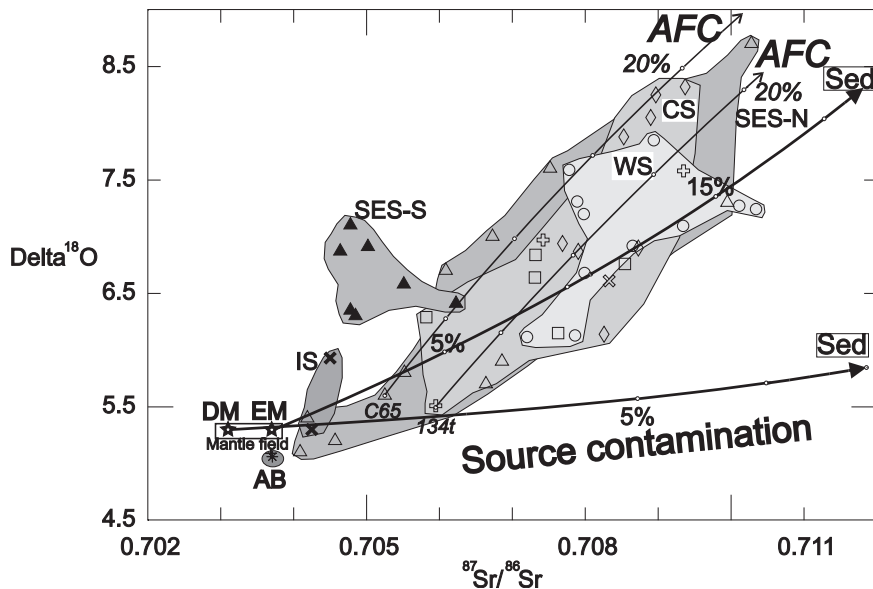


Fig. 8. Petrogenetic modelling—assimilation fractional crystallisation (AFC) and bulk mixing models with average local sediments (Sed)—for Carpathian–Pannonian volcanic rocks using $\delta^{18}\text{O}$ vs. ${}^{87}\text{Sr} / {}^{86}\text{Sr}$ variation. DM ($\delta^{18}\text{O} = 5.3$; ${}^{87}\text{Sr} / {}^{86}\text{Sr} = 0.7031$; Sr = 9 ppm), EM ($\delta^{18}\text{O} = 5.3$; ${}^{87}\text{Sr} / {}^{86}\text{Sr} = 0.7037$; Sr = 66 ppm) and Average Sediments ($\delta^{18}\text{O} = 19$; ${}^{87}\text{Sr} / {}^{86}\text{Sr} = 0.721$; Sr = 175 ppm) is based on Mason et al. (1996). Bulk mixing modelling of DM and EM with average local sediment (Sed) is shown with tick marks for every 5% consumed sediment. For AFC we used $r = 0.4$ trend (degree of assimilation/degree of fractionation), shown with tick marks for every 5% of consumed crust. D_{Sr} is assumed to be 1.2 and in all calculations. Symbols, data and fields as in Fig. 3.

$\delta^{18}\text{O}$ variations make it possible to identify and quantify the crustal contamination effect, giving us a better insight into magma generation revealed by Sr and Nd isotopic variations. Crustal contamination of Western, Central and South-Eastern-N Segments magmas has strongly masked the mantle source processes. According to Fig. 8, South-Eastern-S and Interior Segment magmas do not show significant fractionation or assimilation processes, but rather source heterogeneity and/or source mixing.

4.3. Source contamination processes via slab contribution

The most primitive rocks in the Carpathian–Pannonian area are alkalic basalts (derived from an OIB component mantle) which have the lowest SiO_2 content and narrow range of isotopic variability. In contrast, the most primitive calc-alkaline rocks (up to 56 wt.% SiO_2) show a large isotopic variability considered to be mostly a contribution from the subducted slab (Fig. 7). The most uncontaminated

mantle source of calc-alkaline magmas is that of the primitive South-Eastern-N Segment (Mason et al., 1996), whereas the compositions of Western and Central Segments and some South-Eastern-N Segment magmas indicate a variable, but large contribution from subducted components. Bulk mixing between mantle sources and sediments in O–Sr isotopic modelling produces mixing curves which indicate source contamination of the most primitive magmas in Western and Central Segments and to a lesser extent in South-Eastern-N Segment (Fig. 8). Mixing lines have been constructed between possible mantle (local depleted mantle—DM—and local enriched mantle—EM—after Embey-Isztin et al., 1993; Downes et al., 1995a) and sediment end-members (average value for East Carpathians local sediments from Mason et al., 1996). A pronounced shift of ${}^{87}\text{Sr} / {}^{86}\text{Sr}$ ratio and, with the exception of Beregovo (Central Segment), large $\delta^{18}\text{O}$ variation, suggests source contamination in the range of 1–3% for Sr–O models, using a DM source as the parental composition of magmas from these areas. However, using

an EM source, the amount of contamination required is higher (5–15%) for Beregovo and Tokaj (Central Segment) and Western Segment, where a combination of DM and EM sources is more likely. Differences in $^{87}\text{Sr}/^{86}\text{Sr}$ and $^{143}\text{Nd}/^{144}\text{Nd}$ ratios of the most primitive magmas from South-Eastern Segment, less contaminated, as compared to Western and Central Segments can be interpreted in terms of source contamination via sediment addition (Fig. 6).

The scatter shown by rocks from South-Eastern-S Segment, which lie closer to the bulk mixing line between EM and sediments (Fig. 8), suggests a distinct less contaminated source, which further suffered minor crustal assimilation. The amount of modelled source contamination (up to 15%) suggests a long period and large amounts of sediment subduction in the Western and Central Segments and, to a lesser extent, in Beregovo (Central Segment) and South-Eastern-N Segment volcanic areas. An explanation for the important source enrichment could be long-lived flysch basins which developed during Intracarpathian continental collision since Cretaceous times (Săndulescu, 1984; Roure et al., 1993; Oszczypko, 1998). The compositions of South-Eastern-S Segment mag-

mas suggest mixing processes between more or less contaminated sources, different from the other areas, and favor the interpretation of mixing between relatively high $\delta^{18}\text{O}$ (6–6.9‰) slab-derived melts and a variably enriched mantle source. Two Interior Segment samples show rather depleted Sr and O isotopic ratios, which may be derived from a depleted source (Fig. 8).

Higher LILE/REE and LILE/HFSE ratios are typical features of subduction-related magmas and have been attributed to mass transfer of fluids from the subducted slab into the overlying mantle wedge (e.g. Davidson, 1987; Thirlwall et al., 1996). Because all these elements are highly incompatible during silicate-melt fractionation processes, a diagram of Pb/Nd plotted against $^{143}\text{Nd}/^{144}\text{Nd}$ can be used to distinguish source characteristics (Fig. 9). This approach was used by Vroon et al. (1993) to illustrate a possible scenario with involvement of fluids and sediments in the genesis of calc-alkaline rocks of the Banda arc. The diagram (plotting only the most primitive rocks, up to 56 wt.% SiO_2) indicates that the sources of Western and Central Segments magmas (which have lower $^{143}\text{Nd}/^{144}\text{Nd}$ ratios) can be ex-

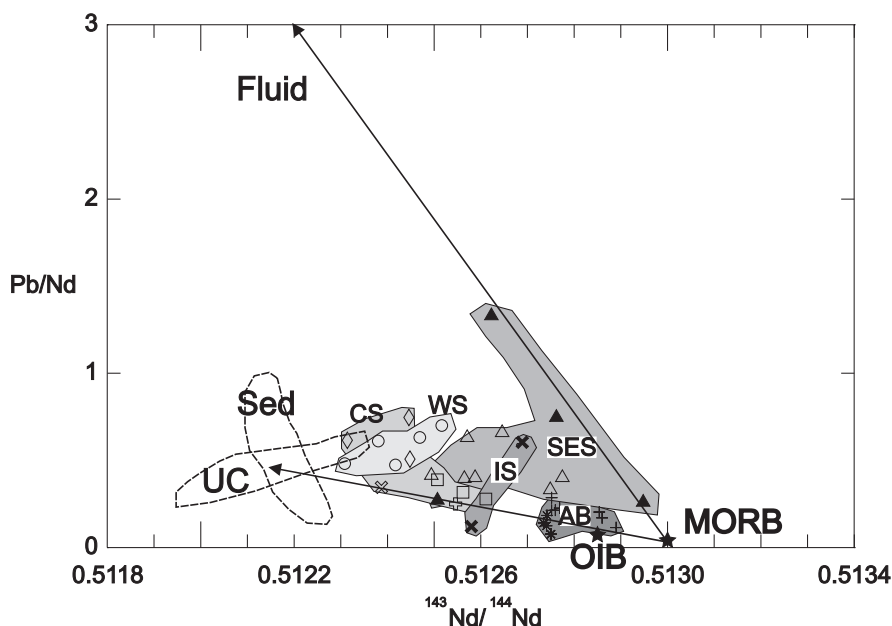


Fig. 9. $^{143}\text{Nd}/^{144}\text{Nd}$ vs. Pb/Nd diagram for most primitive calc-alkaline Carpathian–Pannonian volcanic rocks suggesting a mixing tendency between a MORB–OIB-like sources (according to Sun and McDonough, 1989) and Flysch sediments (Sed) and Upper Crustal rocks (UC) (from Mason et al., 1996). Fluid involvement is also suggested, especially for South-Eastern Segment magmas. Symbols, data and fields as in Fig. 3.

plained as a mixture of sediments with a mantle previously enriched in slab-derived fluids. Only the compositions of Beregovo (Central Segment) and primitive South-Eastern-N Segment magmas suggest small but variable amounts of sediments and fluids involved. Magmas from the South-Eastern-S as well as Interior Segments can be accounted for by an especially large amount of fluid (having also high Ba/La or Ba/Nb ratios).

In summary, trace element and isotopic compositions of the calc-alkaline and related rocks in Carpathian–Pannonian area seem to require contributions of fluids and sediments from the subducted slab to the mantle wedge (with larger amount in Western Segment and Central Segment), which appear to be distinct from crustal assimilation processes.

4.4. Crustal sources versus crustal assimilation

Higher $^{87}\text{Sr}/^{86}\text{Sr}$ values for evolved volcanic rocks of the Carpathian–Pannonian area may reflect assimilation of continental crust (Fig. 6). AFC modelling suggests 5–20% upper crustal assimilation for some intermediary-acid rocks in Western, Central and South-Eastern-N Segments (Fig. 8). However, sometimes they may be evidence for melting of crustal

sources, as in the case of the Bükk rhyolites (Western Segment) or some Tokaj and Gutai rhyolites (Central Segment), which plot inside the local Upper Crust field (Mason et al., 1996) (Fig. 6). The Bükk rhyolites with a high and variable $^{87}\text{Sr}/^{86}\text{Sr}$ at relatively constant SiO_2 (~70 wt.%) probably result from mixing between a crustal source and a differentiated mantle source (see also Fig. 10). Harangi (2001) and Harangi et al. (2001) explained the large $^{87}\text{Sr}/^{86}\text{Sr}$ isotope variation of rhyolites and garnet-bearing andesites in Western Segment by contamination processes via mixing of mantle-derived magmas with variable amounts of lower crustal metasedimentary material. A 20–25% of such metasedimentary material was assumed to produce the garnet-bearing andesites and 40–50% the rhyodacites, process which would not only require a high heat flow (Harangi et al., 2001), but also a considerable amount of metasedimentary lower crustal material.

Evidence for crustal assimilation or derivation from a crustal source is marked by strong enrichment of K_2O over Na_2O , or incompatible LIL elements such as Rb over HFSE such as Zr (e.g. Esperanca et al., 1992) (Fig. 10). Most of the Bükk rhyolites and some rhyolites from Tokaj and Gutai (Central Segment) shift to the right of the calc-alkaline fraction-

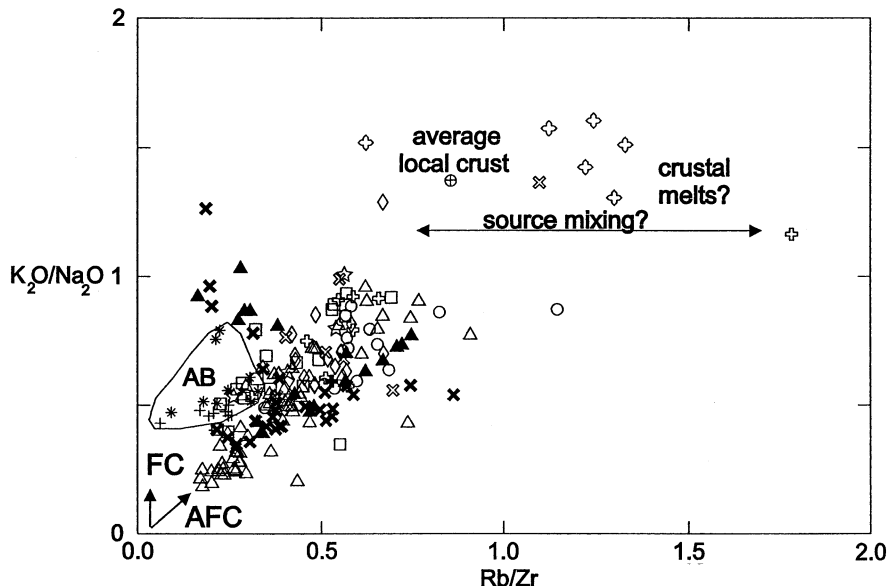


Fig. 10. Rb/Zr vs. $\text{K}_2\text{O}/\text{Na}_2\text{O}$ diagram to distinguish crustal sources from AFC processes in Carpathian–Pannonian volcanic rocks. Average local crust according to Mason et al. (1996). Symbols and data as in Fig. 3.

ation series (AFC), which includes Dej and Beregovo rhyolites (Central Segment) (Szakács, 2000; Seghedi et al., 2001). A different trend from AFC is the increase of K_2O/Na_2O ratio shown by South-Eastern-S as well as Interior SegmentS shoshonites, at lower Rb/Zr and $^{87}Sr/^{86}Sr$, which could suggest a high-K source component. High Rb/Zr is associated with a crustal contribution, via partial melting rather than assimilation, which normally would follow the trend of AFC for the majority of the rocks (Fig. 10). A crustal origin for the Bükk rhyolites (Western Segment) was already suggested by Póka et al. (1998). Their variable Rb/Zr ratios, at similar K_2O/Na_2O ratios, suggest mixing processes, which would involve (1) a dominant acid component derived via crustal partial melting and a (2) component as a result of fractionation and differentiation of a mantle-derived magma.

4.5. Slab-derived melts versus fluid-dominated melting

Slab dehydration commonly contributes fluids to the overlying mantle wedge, promoting melting (Ellam and Hawkesworth, 1988; Tatsumi and Eggins, 1995), whereas slab melting is much more rare. Such melts can react with sub-arc mantle to give rise to adakite magmas (Drummond et al., 1996). The term “adakite” was used firstly by Defant and Drummond (1990) to describe a group of calc-alkaline magmas showing: $SiO_2 \geq 56$ wt.%; $Al_2O_3 \geq 15$ wt.%; $Yb < 1.9$ ppm; $Y < 18$ ppm, $Sr > 400$ ppm; $Sr/Y = 30–300$ and low $^{86}Sr/^{87}Sr$. Adakites were first interpreted as the result of partial melting of hot, subducted oceanic crust (Defant and Drummond, 1990) and later as a result of reaction between such slab-derived melts and the mantle wedge (Drummond et al., 1996). However, it is difficult to differentiate clearly between melting due to fluid-related enrichment and slab-melt enrichment in the generation of calc-alkaline magmas by melting in the mantle wedge, as the two processes result in similar geochemical features (Kapezhinskas et al., 1997; Castillo et al., 1999). Besides young and hot subducted slabs, which were first thought to produce adakites (Defant and Drummond, 1990), a number of other tectonic processes appear to be able to produce adakites. These include remnant slabs, oblique or fast subduction, arc–arc-collision, initia-

tion of subduction, slab-tears, flat subduction, slab windows and whenever the edge of a subducting plate is warmed or ablated by mantle flow (Petford and Atherton, 1995; Defant and Kapezhinskas, 2001; Yagodzinski et al., 2001).

The Y–Sr/Y plot (Defant and Drummond, 1990) is commonly used to differentiate adakite magmas from typical calc-alkaline magmas (Fig. 11). Sr behaves incomparably in high-pressure partial melting of basalts due to the absence or instability of plagioclase, whereas Y is controlled by garnet in the residuum (Drummond et al., 1996). Most of the samples from South-Eastern-S and Interior Segments plot in the adakite field in Fig. 11, although some (mostly from Interior Segment) have slightly higher Y contents, which causes them to plot slightly outside of the recognised field of adakite magmas. Other important signatures indicating an adakite-like character of most Interior and South-Eastern-S Segments magmas are their low $^{86}Sr/^{87}Sr$ ratios (ca. 0.7045), with higher K_2O and Rb (for South-Eastern-S Segment) and relatively high in Cr and Ni contents (Mason et al., 1996; Roşu et al., 2001). In South-Eastern-S Segment these characteristics were initially thought to relate to melt extraction processes (Seghedi et al., 1987; Szakács et al., 1993) or considered to be a result of efficient dehydration of the subducted lithosphere in a hotter subduction regime due to mantle upwelling (Mason et al., 1996, 1998). An alternative hypothesis to slab-melting for the Interior Segment magmas would involve partial melting of garnet-bearing lower crust or mantle lithosphere related to crustal extension or lower-crustal delamination (e.g. Atherton and Petford, 1993; Petford and Atherton, 1995; Xu et al., 2002), or mixing of mantle-derived magmas with lower crustal melts (Davidson et al., 1990). It seems, however, that the understanding of the tectonic context of adakite and adakite-like magma genesis is still incomplete (Yagodzinski et al., 2001).

4.6. Identification of primary mantle sources

The most primitive rocks in the Carpathian–Pannonian area, represented by alkalic and calc-alkaline basalts and basaltic andesites, give the best insight into the issue of mantle sources. Previous studies have shown that alkalic basalts represent partial melts of an

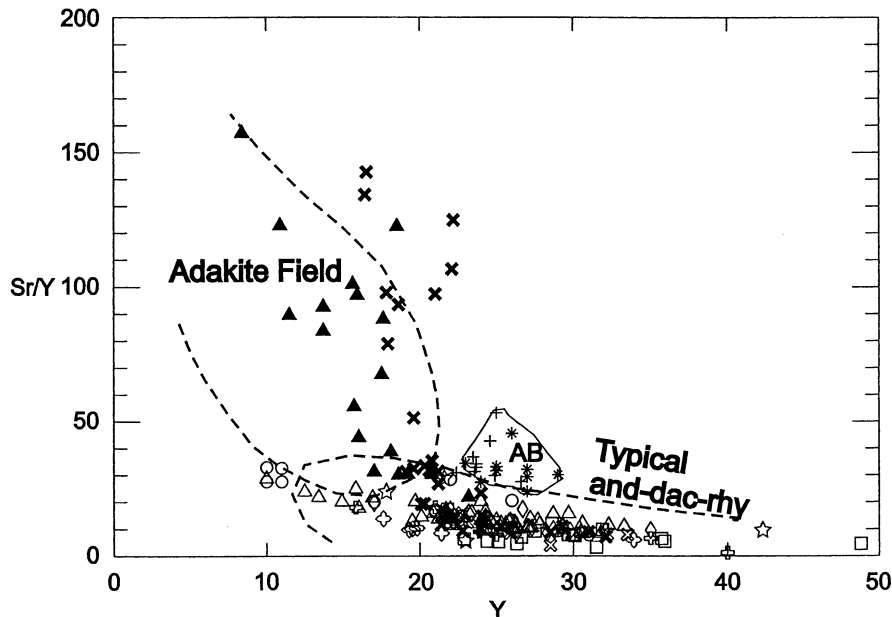


Fig. 11. Y – Sr/Y plot (after Defant and Drummond, 1990) to differentiate adakite-like magmas from typical calc-alkaline magmas. Symbols and data as in Fig. 3.

asthenospheric mantle with little contribution from the lithosphere, whereas calc-alkaline basalts were extracted from a subduction-modified asthenospheric mantle (e.g. Salters et al., 1988; Embey-Isztin and Dobosi, 1995; Rosenbaum et al., 1997). Spinel lherzolite and pyroxenite xenoliths carried by alkalic basalts were interpreted as representing lithospheric mantle (Downes and Vaselli, 1995; Vaselli et al., 1995; Chalot-Prat and Boulier, 1997). Depleted mantle geochemistry characterises the Eastern Transylvanian Basin (Perşani Mts.) lithosphere, which does not show important interaction with subduction-zone fluids, but an enrichment due to infiltration of alkaline melts (Vaselli et al., 1995). Lithospheric mantle in the central part of the Pannonian Basin displays evidence of subduction-related enrichment by silicate melts and aqueous fluids (Rosenbaum et al., 1997). However, the relatively refractory nature of the lithospheric mantle would preclude it as a major source for basaltic magmas (Downes et al., 1995b; Downes and Vaselli, 1995).

Ratios of high field strength elements (HFSE) such as Nb and Zr can provide insight into variations in magma source composition (e.g. Davidson, 1996; Singer et al., 1996). Nb and Zr are depleted in

subduction-related magmas and are assumed to be dominantly mantle-derived, being relatively immobile under hydrothermal conditions and strongly fractionated only during melting or magma-mixing processes (Thirlwall et al., 1994; Davidson, 1996). However, it has been suggested that during mantle enrichment processes Nb and Zr may be added to the mantle source (Pearce and Parkinson, 1993). The Nb/Zr ratios are not affected by fractional crystallisation in relatively mafic magmas and are largely unaffected by crustal contamination. The Nb/Zr–Nb diagram for most primitive rocks (< 56 wt.% SiO₂) (Fig. 12) shows Zr–Nb values starting from ~ 0.05 (close to a typical MORB value) up to 0.20, which is closer to OIB. Different Nb/Zr ratios are generally interpreted in terms of variations in source composition and/or changes in degree of partial melting of the mantle (e.g. Thirlwall et al., 1994; Singer et al., 1996). In terms of source variation, calc-alkaline volcanic rocks from South-Eastern-N Segment are closer to a MORB-like source than those of Western and Central Segments, while South-Eastern-S and Interior Segments and part of Beregovo and Tokaj (Central Segment) are closer to an OIB influence (Fig. 12). Alternatively, large Nb/Zr variation could be interpreted as variable degrees

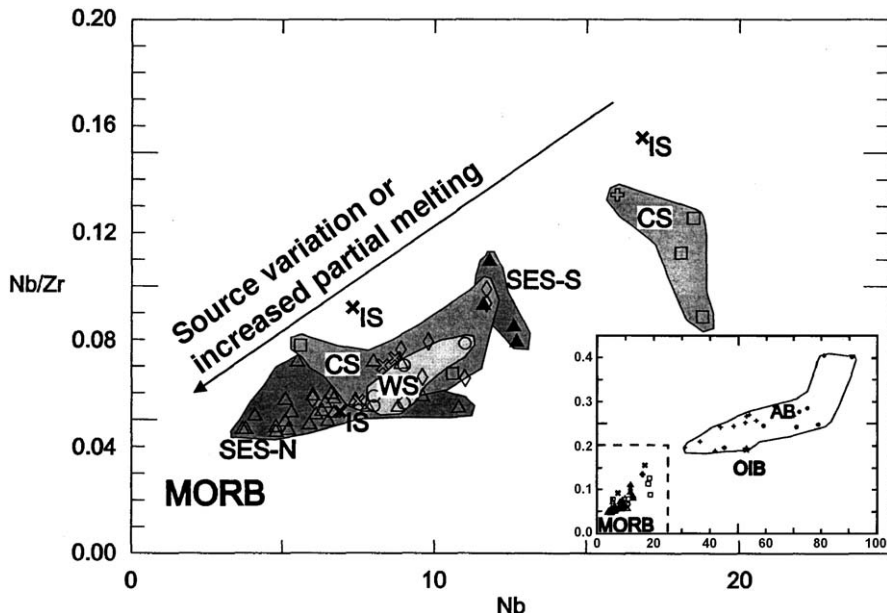


Fig. 12. Nb/Zr vs. Nb diagram for most primitive calc-alkaline Carpathian–Pannonian volcanic rocks. MORB and OIB after Sun and McDonough (1989). Symbols, data and fields as in Fig. 3.

of melting, as might be the case for the Interior Segment magmas.

A plot of Th/Y vs. Nb/Y (Fig. 13) also gives constraints on different mantle source components. The Nb/Y ratio can be used to differentiate between mantle sources, whereas Th/Y can be used to monitor the transfer of slab-derived components to the mantle wedge, because it is probably transferred via subducted sediments (e.g. Elliot et al., 1997; Peate et al., 1997). The alkalic basalts, which represent local asthenospheric OIB-like source (Embel-Isztin et al., 1993; Dobosi et al., 1995; Downes et al., 1995a; Harangi et al., 1995), clearly plot in a separate field around OIB. Most South-Eastern-N Segment samples are again closer to the N-MORB source, whereas other samples become more and more enriched relative to N-MORB, the closest to OIB being those from South-Eastern-S Segment, Beregovo, Tokaj (Central Segment) and Interior Segment. Variable Nb/Y ratios may reflect mantle wedge enrichment by an OIB component, evident for the Beregovo and Tokaj volcanic areas (Central Segment) and South-Eastern-S. Increased Th/Y ratios between 0.01 and 0.1 can be attributed to mass transfer from the subducted slab to the overlying mantle wedge (Peate et al., 1997), as

is the case for magmas from the Western Segment and Central Segment. In contrast, magmas from the Interior Segment that have high and variable Th/Y and Nb/Y ratios were derived from different and heterogeneous sources, probably of lithospheric and/or lower crustal origin. Such variation is not compatible with a small-scale homogeneous source, as the asthenospheric mantle it is expected to be.

The source mixing model for the origin of Carpathian–Pannonian calc-alkaline magmas using Zr/Nb ratio versus $^{87}\text{Sr}/^{86}\text{Sr}$ will assume simple bulk mixing between N-MORB-source and local OIB-source components and averaged local sediments from the East Carpathians (Mason et al., 1996) (Fig. 14). This is workable since the Zr/Nb ratio is rather insensitive to fluid fractionation and closely approaches the ratios of the sediments and/or mantle components. Binary mixing curves between either of the mantle sources and local sediments do not fit the volcanic rocks (< 56 wt.% SiO₂). Therefore three components must be implicated. The presence of an OIB-like component is most obvious in the Tokaj and Beregovo areas (Central Segment) and South-Eastern-S Segment, whereas source contamination and/or mixing processes between mantle and crustal magmas characterises

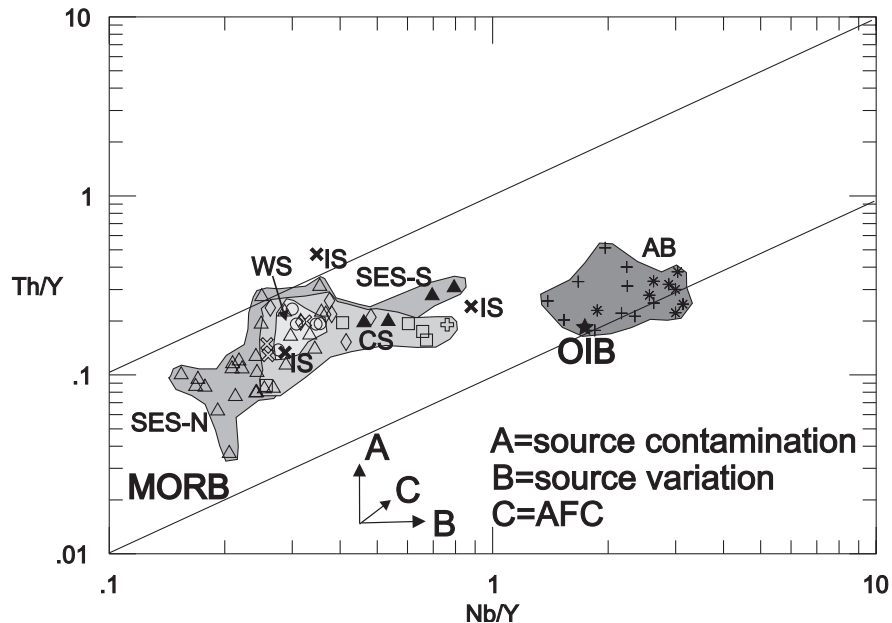


Fig. 13. Nb/Y vs. Th/Y diagram for most primitive calc-alkaline Carpathian–Pannonian volcanic rocks. MORB and OIB after Sun and McDonough (1989). Symbols, data and fields as in Fig. 3.

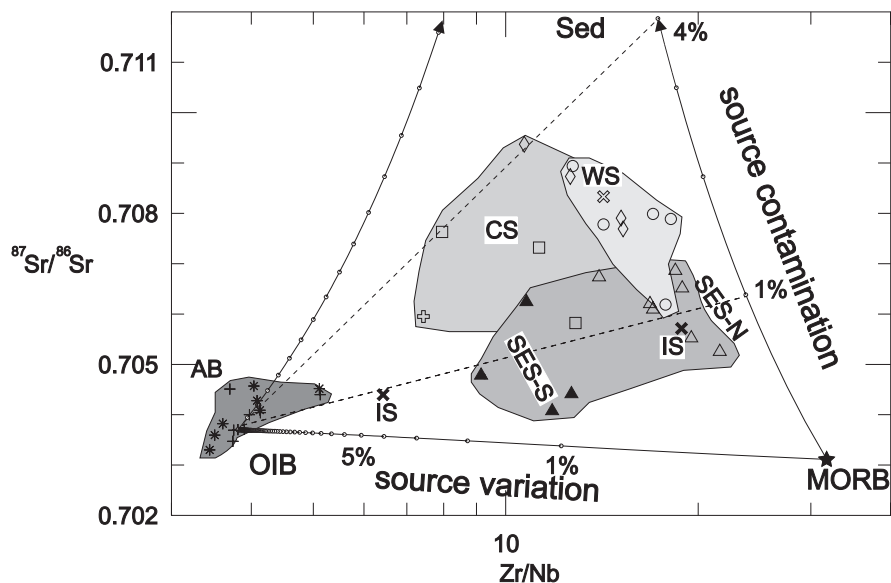


Fig. 14. Zr/Nb vs. $^{87}\text{Sr}/^{86}\text{Sr}$ for Carpathian–Pannonian volcanics showing binary source bulk mixing models between N-MORB (according to Sun and McDonough, 1989) and local OIB-like source ($\text{Zr}/\text{Nb} = 3.8$; $^{87}\text{Sr}/^{86}\text{Sr} = 0.7036$ according to Downes et al., 1995a; Embey-Isztin et al., 1993; Harangi et al., 1995) and an average of East Carpathians sediments ($\text{Zr}/\text{Nb} = 2$; $^{87}\text{Sr}/^{86}\text{Sr} = 0.721$, from Mason et al., 1996). Symbols, data and fields as in Fig. 3.

Western and Central Segments magmas. The large scattered distribution of the Interior Segment magmas, in contrast to the other areas, at rather low $^{87}\text{Sr}/^{86}\text{Sr}$, again suggests source heterogeneity and/or mixing processes between more or less contaminated sources.

The mantle-source discrimination diagrams (Figs. 12–14) suggest that a compositionally heterogeneous mantle ranging from MORB-like to OIB-like sources was present below the Carpathian–Pannonian region. Rosenbaum et al. (1997) suggested that the asthenospheric mantle became heterogeneous by variable infiltration of a HIMU-mantle plume component, prior to the onset of subduction in the Miocene. We admit pre-Miocene subduction-related source heterogeneity, but additionally we relate mantle heterogeneity along all the segments to strong disturbances by ascent of hot asthenospheric mantle (OIB-like) caused by rollback processes and/or breakoff, or extensional processes in a continuous sequence of events which outline the Miocene evolution of Carpathian–Pannonian region (e.g. Nemčok et al., 1998; Seghedi et al., 1998).

5. Implications of geochemical data for geodynamic evolution of the region

5.1. Relative role of subduction and back-arc extension

The Carpathian–Pannonian area has experienced both subduction and extension during Miocene–Quaternary times (Royden, 1988; Horváth, 1993; Csontos, 1995). Back-arc extension occurred during Early Miocene block collision due to the uneven rollback of the subduction zone (Royden and Burchfiel, 1989). This caused crustal thinning in the Pannonian basin, mostly along the mid-Hungarian belt, where the Alcapa and Tisia blocks were in contact since the Early Miocene. The rotation of the two blocks in opposite senses may have also contributed to crustal thinning. Csontos and Nagymarosy (1998) suggested that rotation around the external rotation poles of the two major blocks led to extensional deformation along the mid-Hungarian belt, causing tangential extension, lithosphere thinning and generation of wedge-shaped triangular basins. Doglioni et al. (1999) pointed out that W-directed subduction zones show slab rollback,

whereas E-directed subduction zones show much lower angles of subduction, which was interpreted in terms of relative eastward mantle flow or westward drift of the lithosphere. The W-directed Miocene subduction zone of the Carpathians is not an exception to this observation, evidenced by slab-rollback, which is due not only to slab pull (Royden, 1993), but also to eastward mantle flow or opposite drift of the European Plate (Doglioni et al., 1999).

We will now consider the relationship between extension and volcanism. Most of the Western Segment volcanism (20–11 Ma) generated in the Alcapa Block is attributed to back-arc extension, at its initial stage being represented by “areal-type silicic volcanics” and in the intense back-arc extension stage by “areal-type andesitic volcanics” (Lexa and Konečny, 1998). Most of this volcanism was directly associated with Miocene sedimentation in the Pannonian basin (Vass, 1995; Kováč et al., 1998). Early Miocene silicic volcanism was also generated in extensional basins along the southern border of the Central Western Carpathians (e.g. Western Segment rhyolites), while the Middle Miocene volcanism was a response to the transtension and extension around the Transcarpathian basin (e.g. Central Segment rhyolites) (Lexa and Konečny, 1998; Seghedi et al., 1998; Seghedi et al., 2001). Our geochemical study supports the different features of the Early Miocene back-arc acid lavas (e.g. Western Segment rhyolites) as compared to Middle Miocene acid lavas (Central Segment rhyolites). The older rhyolites show a larger crustal melt contribution compared to the younger ones. Furthermore, some of the younger rhyolites (e.g. Beregovo, from Central Segment) represent fractionated products of a mantle source variable enriched in OIB-like components, as a result of perturbed asthenospheric influx adjoined to the bending of the slab (Downes et al., 1995b; Seghedi et al., 2001). The change in the back-arc evolution in front of the Alcapa block, also suggested by lateral depocenter migration, probably corresponds to changes in the rollback-induced pull at the front (Meulenkamp et al., 1996). During Early Miocene times, slab pull and mantle flow provoked northeastward transport and counter-clockwise rotation of the Alcapa block (Márton, 1987), causing back-arc extension at the southern border of the Central Western Carpathians. Large volumes of extruded calc-alkaline products during

this period (18–16 Ma) suggest that subduction rate-rollback must have been important as well as generation and rapid ascent of the magmas in a regional tensional stress regime. Subsequently, during Middle Miocene times (~ 16 Ma), the system evolved by a rapid shift of overall extension in the Transcarpathian basin. This extension suggests a change in the direction of pull of the northeastern part of Alcapa block (Zemplin block) in a northeastward motion (Meulen-kamp et al., 1996) and counterclockwise rotation (Pătrașcu et al., 1994; Panaiotu, 1998; Márton et al., 2000). This change in direction was coeval with the eastward translation and fast clockwise rotation of the Tisia block between 14.5 and 12 Ma (Csontos, 1995; Panaiotu, 1999). Extension of Tisia does not show any back-arc development. Instead, basins showing NW–SE trending graben-like features (Royden, 1988) are responsible for the generation of a special type of extension-related magmatism (including adakite-like calc-alkaline type) in the Apuseni area (Roșu et al., 2001). These basins could be related to thinning of the lithosphere at the external hinge (along the mid-Hungarian belt) during counterclockwise rotation around a pole situated in western Moesia (Csontos and Nagymarosy, 1998) and/or en-echelon brittle crustal deformations during fast clockwise rotation (Fig. 2).

5.2. Source variability

We will now attempt to integrate the main conclusions of this study to refine regional tectonomagmatic models (e.g. Csontos, 1995; Lexa and Konečny, 1998; Seghedi et al., 1998; Harangi, 2001). Magmatism started in Lower Miocene times and continued into the Plio-Pleistocene, significantly later than the perceived end of basin closure and subduction along the Inner Carpathian arc (Royden and Burchfiel, 1989). To produce calc-alkaline magmatism it is necessary to have subduction-induced metasomatism of the asthenospheric or lithospheric mantle (Green and Ringwood, 1968; Tatsumi and Eggin, 1995). Temporal and spatial changes of volcanic activity can be related to variations of the critical tectonic processes responsible for melt generation. Thus, as subduction was responsible for the calc-alkaline magmatism, then the subducted slab must have reached the depth of magma generation of 100–

120 km (Gill, 1981; Sekine and Willey, 1982). Significantly, in the Carpathian–Pannonian region, the climax of calc-alkaline magmatism occurred in a sequence of events after the main period of convergence related to subduction, controlled by rollback processes and subsequent breakoff of the slab (e.g. Csontos, 1995; Nemčok et al., 1998; Seghedi et al., 1998). However, the relationship between the timing of subduction metasomatism and the climax of magmatism still remains a matter of debate in the region.

Here we will follow the space–time distribution of volcanic areas with respect to block distribution (according to Seghedi et al., 1998) and try to suggest their possible relationships to geodynamic processes. Along the Western Segment collision was an early Middle Miocene event, marked by counterclockwise rotations of the Alcapa block (e.g. 80–90° during 21–18.5 Ma and 30° during 17.5–16 Ma) (Pécskay et al., 1995a; Márton and Pécskay, 1998), roughly contemporaneous with generation of the oldest rhyolitic–andesitic volcanism. The earliest magmas were generated above the downgoing slab, which passed through the magma generation window at the inception of the back-arc extension period. Long-term subduction caused important source contamination. Diapiric uprise of large-volume partial melts from the contaminated mantle caused underplating and crustal anatexis, leading to mixing of crustal melts with mantle-derived magmas (e.g. Bükk rhyolites). The rate of subduction, followed by rollback, matched the rate of convergence (~ 2 cm year⁻¹, according to Roca et al., 1995). This situation favored long-residence differentiation of mantle-derived magmas in crustal magma chambers and sometimes mixing with crustal melts. The 20–10 Ma volcanism associated with the Alcapa block, characterized by eruption of large volume intermediate and silicic magmas, suggests the presence of a large volume of underplated magmas. Increasing magma supply rate, associated with rising geothermal gradients, lead to partial anatexis of the crust. In a regional compressional stress regime that generally favored storage of silicic and intermediate magmas, crustal rotations may have led to localized extension that permitted eruption. From deep level magma chambers the fractionated silicic magmas rose to the surface, sometimes followed by andesitic magmas (Pécskay et al., 1995a; Lexa and Konečny, 1998; Nemčok et al., 1998; Harangi et al.,

2001). General northward younging of the calc-alkaline magmatism in the Western Segment (Pécskay et al., 1995a; Lexa and Konečny, 1998) suggests a relationships with rollback and back-arc extension (Lexa et al., 1995; Huismans et al., 2001) and/or delamination processes (de Boorder et al., 1998; Seghedi et al., 1998). After cessation of calc-alkaline magmatism at ~ 10 Ma, further asthenospheric alkaline volcanism occurred, suggesting local asthenospheric upwelling and related adiabatic partial melting of an OIB-like source (Embey-Isztin et al., 1993; Dobosi et al., 1995; Harangi et al., 1995; Konečny et al., 1995).

In front of the Central Segment collision ended in upper Middle Miocene times with simultaneous counterclockwise rotation of the easternmost Alcapa lithospheric block (Zemplín) (Panaiotu, 1998; Márton et al., 2000) and clockwise rotation of Tisia in direct relationship with a change in direction (toward northeast) of the slab pull. Volcanism was active mainly between 15 and 8 Ma, in a large area in front of the Zemplín block, facilitated by a complex extensional–transtensional regime. At the same time, in front of the Tisia block a transpressive regime around the Dragoš Voda fault (Zweigel, 1997) precluded extrusive volcanism, so the magmatic activity consisted of shallow-level intrusions.

The calc-alkaline magmas erupted in front of the Zemplín block were generated by important source contamination of the asthenosphere during slab rollback of the subducted lithosphere, directly related to collisional processes, thermal disturbance caused by ascent of hot asthenospheric mantle during the late-stage back-arc opening and rotations of the Intracarpathian blocks. Eruptions were facilitated by strike-slip faults (e.g. Csontos, 1995; Seghedi et al., 1998, 2001). Rollback and breakoff processes support a trench-ward asthenospheric influx and consequently a thermal input, which allowed almost concomitant generation of calc-alkaline magmas all along the back-arc and trench (Seghedi et al., 1998, 2001; Kovacs, 2002).

In front of the Tisia block, during subduction rollback, the mantle wedge was perturbed and contaminated. Magmas were formed by melting of a heterogeneous mantle wedge or lower crust and were transported to the surface along the strike-slip fault system. Volcanic activity within the Central Segment at 15–8 Ma may have followed the arrival of unsub-

ductable continental crust of the European Platform (Tornquist–Teisseyre zone), and was probably followed by breakoff processes (Nemčok et al., 1998; Seghedi et al., 1998; Wortel and Spakman, 2000). This segment is a remarkable example of subduction-related rollback magmatism (rollback of a normal slab followed by back-arc extension and almost simultaneous breakoff processes), by its position closest to the accretionary prism and its distinctive and complex geochemical features (e.g. large mantle source variation in back-arc setting and larger fluid-induced metasomatism source enrichment and assimilation in high-level magma chambers toward the trench).

Along the South-Eastern Segment, post-collisional volcanism developed at 10 Ma and continued to <1 Ma, behind and along the Carpathian accretionary prism. It was most probably related to upper Middle Miocene oblique subduction and rollback bending of a narrow slab (Mason et al., 1998), which created the necessary tectonic conditions for magma generation. A tear may have progressed along the slab as breakoff progressed from north to south. Migration of magmatic activity from north to south may be explained by a corresponding migration of the magma-generating zone along the arc (Mason et al., 1998). In the extreme south of the segment, magmas were generated by melting of subducted oceanic crust in the eclogite field (adakite-like magmas) due to increased temperature by mantle upwelling during late stage of a complex oblique subduction breakoff processes. Breakoff and tearing of the slab at shallow levels (<50 km) in the extreme south of the arc and strike-slip tectonics, accompanied by an extensional stress regime at the surface of the upper plate (Gîrbacea and Frisch, 1998; Ciulavu, 1999; Matenco and Bertotti, 2000), may account for some of the unusual geological features (e.g. contemporaneous eruption of normal and adakite-like calc-alkaline, alkaline, and alkalic basaltic magmas. We suggest that this segment is a special case of subduction-related rollback magmatism (rollback of an oblique slab and further along-arc breakoff and tearing processes). Recently, Chalot-Prat and Gîrbacea (2000), based on Gîrbacea's (1997) geotectonic model, suggested the generation of both calc-alkaline and alkalic basaltic magmas by intra-mantle delamination of lower European plate and not from overriding plate mantle, but this is not supported by geochemical data (Mason et al., 1996; this work)

or other geodynamic models (e.g. Maťenco, 1997; Mason et al., 1998; Seghedi et al., 1998).

Although it displays trace element and isotopic signatures similar to subduction-related magmatism, the location of calc-alkaline volcanism in the Interior Segment, far behind the volcanic front, is not consistent with a contemporaneous subduction model. In the Apuseni area there is a transition from typical calc-alkaline to adakite-like calc-alkaline magmas developed at 15–8 Ma, which was a period of major rotations and rollback processes and generation of magmas in Central Segment. The adakite-like features are more and more evident between 12 and 8 Ma, after the cessation of the large clockwise rotations (Roşu et al., 1997, 2001; Szakács et al., 1999). Close to the Apuseni area the presence of ~2.5 Ma alkalic basalts and ~1.5 Ma shoshonites suggests a hot mantle upwelling in a local extensional environment. The Apuseni magmatism was generated in an extensional regime (Royden, 1988; Csontos and Nagymarosy, 1998; Ciulavu, 1999) and was related to decompressional melting during eastward translation and clockwise rotation of the Intracarpathian blocks during Middle Miocene (Seghedi et al., 1998; Roşu et al., 2001). An extensional regime which would favor decompressional melting and further OIB-like mantle upwelling could increase the thermal regime to generate normal to adakite-like calc-alkaline melts by partial melting of an already enriched lithospheric mantle (presumably in previous Alpine subduction events) and/or lower crust (Balintoni and Vlad, 1998; Seghedi et al., 1998; Roşu et al., 2001).

6. Conclusions

We suggest that Neogene–Quaternary kinematics of Intracarpathian blocks (Alcapa and Tisia) were responsible for specific geochemical features and evolution of the magmas of the Carpathian–Pannonian area. Calc-alkaline and alkalic magmatism was closely related to W-directed subduction, rollback and extensional processes. In accordance to the spatial distribution of the magmatic activity, the following segments were distinguished: Western Segment, Central Segment, South-Eastern Segment and Interior Segment.

In the Western Segment, collision was an early Middle Miocene event, marked by counterclockwise

rotations of the Alcapa block and subduction-retreat-related back-arc extension. Magmas were generated above the downgoing slab, which passed through the magma generation window during the back-arc extension period. Uprise of diapiric asthenospheric partial melts affected by long-term fluid and sediment contamination, caused underplating and crustal anatexis, and mixing of crustal melts with mantle-derived magmas. From deep crustal magma chambers the fractionated silicic magmas rose to the surface accompanied by andesitic magmas.

Within the Central Segment collision ended in upper Middle Miocene times during clockwise rotation of the Tisia block and almost simultaneous counterclockwise rotation of the northeasternmost part of Alcapa (Zemplin block) in direct relationship with rollback and further breakoff of the subducted slab. Calc-alkaline magmas were generated by fluid and sediment contamination of the asthenosphere, following subduction and slab rollback, directly related to collisional processes. Thermal disturbance due to ascent of small-scale hot asthenospheric mantle (causing large mantle source variation), during a second phase of extension (Huismans et al., 2001), facilitated simultaneous eruption of the magmas within a large area (from trench-arc to back-arc). This segment could be characterised as subduction-related rollback magmatism.

Along the South-Eastern Segment post-collisional volcanism can be explained by upper Middle Miocene oblique subduction and rollback of a narrow landlocked oceanic remnant basin in front of the Tisia block, which created the necessary tectonic conditions for breakoff processes and magma generation, being a particular case of subduction-related rollback magmatism. Breakoff progressed along the slab from north to south, as suggested by the migration of magmatic activity in the same direction, and explained by a corresponding migration of the magma-generating zone along the arc. AFC processes were important at various crustal levels. In the extreme south of the arc, breakoff and tearing of the slab at shallow levels (~50 km) and strike-slip tectonics, accompanied by an extensional stress regime may account for some of the unusual magma-generating conditions in this segment (e.g. contemporaneous eruption of typical calc-alkaline and adakite-like calc-alkaline, shoshonitic and alkalic basaltic magmas).

Calc-alkaline volcanics of the Interior Segment (mostly the Apuseni Mountains magmatism) located ~ 200 km behind the Central Segment volcanic front, but contemporaneous with it, are inconsistent with a typical subduction model. The temporal transition from typical calc-alkaline to adakite-like calc-alkaline magmas, as well as the lack of important AFC processes, is assumed to be related to decompressional melting of the lower crust and/or of the enriched lithospheric mantle in an extensional regime during eastward translation and fast clockwise rotation of the Tisza block during Middle Miocene times.

The Late Miocene–Quaternary alkalic basaltic magmas have an asthenospheric origin (OIB-like) being generated in various local extensional conditions. The origin of calc-alkaline magmas was very complex and related to various processes developed in the mantle and crust. The most primitive calc-alkaline magma compositions suggest involvement of three components: N-MORB source, OIB source and various amounts of subduction-related components. Mantle contamination is an important process in Western and Central Segments, since source variation is important in Central and Interior Segments. Differentiation processes took place mostly at high crustal levels via assimilation-fractional crystallisation processes (AFC) in South-Eastern-N and Central Segments. Adakite-like calc-alkaline magmas were generated in conditions of fluid-related melting via slab melting (South-Eastern-S Segment) or decompressional melting (Interior Segment) of lithospheric mantle and/or lower crust. Various mixing processes such as between mantle-derived differentiated magmas and crustal melts (e.g. Western Segment rhyolites) or between various sources (e.g. South-Eastern-S and Interior Segment S) complicate the petrogenetic history.

Acknowledgements

We are grateful to the Royal Society for financial support of our joint project. The Institute of Nuclear Research of the Hungarian Academy of Sciences, the Geological Institute of Romania and the Central Research Fund of the University of London are thanked for fieldwork support for their scientists. The University of London Intercollegiate Research Service and a grant from Birkbeck College Research Fund

made the analytical work possible. We thank Andy Beard, Giz Mariner, Claire Grater, Gerry Ingram and Dave Mattey for their technical assistance with geochemical analyses. We thank EUROPORBE for useful discussions in many PANCARDI workshops. We thank Olav Eklund and Gábor Dobosi for their constructive reviews and Steve Foley for his pieces of advice.

References

- Atherton, M.P., Petford, N., 1993. Generation of sodium-rich magmas from newly underplated basaltic crust. *Nature* 362, 144–146.
- Balintoni, I., Vlad, S., 1998. Tertiary magmatism in the Apuseni Mountains and related tectonic setting. *Stud. Univ. Babeş-Bolyai, Geol.* IX, 1–11.
- Castillo, P.R., Janney, P.E., Solidum, R.U., 1999. Petrology and geochemistry of Camiguin Island, southern Philippines: insight to the source of adakites and other lavas in a complex arc setting. *Contrib. Mineral. Petrol.* 134, 33–51.
- Chalot-Prat, F., Boulier, A.-M., 1997. Metasomatism in the subcontinental mantle beneath the Eastern Carpathians (Romania): new evidence from trace element geochemistry. *Contrib. Mineral. Petrol.* 129, 284–307.
- Chalot-Prat, F., Gîrbacea, R., 2000. Partial delamination of continental mantle lithosphere, uplift-related crustal–mantle decoupling, volcanism and basin formations: a new model for the Pliocene–Quaternary evolution of the southern East Carpathians, Romania. *Tectonophysics* 327, 83–107.
- Ciulavu, D., 1999. Tertiary tectonics of the Transylvanian basin. PhD thesis. Vrije Universiteit, Faculty of Earth Sciences, Amsterdam. 154 pp.
- Csontos, L., 1995. Tertiary tectonic evolution of the Intra-Carpathian area: a review. *Acta Vulcanol.* 7, 1–13.
- Csontos, L., Nagymarosy, A., 1998. The mid-Hungarian line: a zone of repeated tectonic inversion. *Tectonophysics* 297, 51–71.
- Csontos, L., Nagymarosy, A., Horvath, F., Kováč, M., 1992. Tertiary evolution in the Intracarpatican area: a model. *Tectonophysics* 208, 221–241.
- Davidson, J.P., 1987. Crustal contamination versus subduction zone enrichment: examples from the Lesser Antilles and implications for mantle source compositions of island arc volcanic rocks. *Geochim. Cosmochim. Acta* 51, 2185–2198.
- Davidson, J.P., 1996. Deciphering mantle and crustal signature in subduction zone magmatism. In: Bebout, G.E., Scholl, D.W., Kirby, S.H., Platt, J.P. (Eds.), *Subduction Top to Bottom*. Geophysical Monograph, vol. 96, pp. 251–262.
- Davidson, J.P., McMillan, N.J., Moorbath, S., Worner, G., Harmon, R.S., Lopez-Escobar, L., 1990. The Nevados de Pavachata volcanic region, 18°S/69°W, N Chile, II. Evidence for widespread crustal involvement in Andean magmatism. *Contrib. Mineral. Petrol.* 105, 412–443.
- de Boorder, H., Spakman, W., White, S.H., Wortel, M.J.R., 1998.

- Late Cenozoic mineralization, orogenic collapse and slab detachment in the European Alpine Belt. *Earth Planet. Sci. Lett.* 164, 569–575.
- Defant, M.J., Drummond, M.S., 1990. Derivation of slab arc magmas by melting of young subducted lithosphere. *Nature* 347, 662–665.
- Defant, M.J., Kapezinskis, P., 2001. Evidence suggests slab melting in arc magmas. *EOS Trans. AGU* 82 (6), 65–69.
- Dobosi, G., Fodor, R.V., Goldberg, S.A., 1995. Late Cenozoic alkalic basalt magmatism in Northern Hungary and Slovakia: petrology, source composition and relationships to tectonics. *Acta Vulcanol.* 7, 199–207.
- Dobosi, G., Downes, H., Matthey, D., Embey-Isztin, A., 1998. Oxygen isotope ratios of phenocrysts from alkali basalts of the Pannonian basin: evidence for an O-isotopically homogeneous upper mantle beneath a subduction-influenced area. *Lithos* 42, 213–223.
- Doglioni, C., Harabaglia, P., Merlini, S., Mongelli, F., Peccerillo, A., Piromallo, C., 1999. Orogenes and slabs vs. their direction of subduction. *Earth-Sci. Rev.* 45, 167–208.
- Downes, H., Seghedi, I., Szakacs, A., Dobosi, G., James, D.E., Vaselli, O., Rigby, I.J., Ingram, G.A., Rex, D., Pécskay, Z., 1995a. Petrology and geochemistry of the late Tertiary/Quaternary mafic alkaline volcanism in Romania. *Lithos* 35, 65–81.
- Downes, H., Pantó, Gy., Póka, T., Matthey, D.P., Greenwood, P.B., 1995b. Calc-alkaline volcanics of the Inner Carpathian arc, Northern Hungary: new geochemical and oxygen isotopic results. *Acta Vulcanol.* 7, 29–41.
- Downes, H., Vaselli, O., 1995. The lithospheric mantle beneath the Carpathian–Pannonian region: a review of trace element and isotopic evidence from ultramafic xenoliths. *Acta Vulcanol.* 7, 219–231.
- Drummond, M.S., Defant, M.J., Kapezhinskis, P.K., 1996. Petrogenesis of slab-derived trondhjemite–tonalite–dacite–adakite magmas. *Trans. R. Soc. Edinb. Earth Sci.* 87, 205–215.
- Ellam, R.M., Hawkesworth, C.J., 1988. Elemental and isotopic variation in subduction related basalts: evidence for three component model. *Contrib. Mineral. Petrol.* 98, 72–80.
- Ellam, R.M., Harmon, R.S., 1990. Oxygen isotope constraints on the crustal contribution to the subduction-related magmatism of the Aeolian Islands, southern Italy. *J. Volcanol. Geotherm. Res.* 44, 105–122.
- Elliot, T., Plank, T., Zindler, A., White, W., Bourdon, B., 1997. Element transport from slab to volcanic front at the Mariana arc. *J. Geophys. Res.* 102, 14991–15019.
- Embey-Isztin, A., Dobosi, G., 1995. Mantle source characteristics for Miocene–Pleistocene alkali basalts, Carpathian–Pannonian region: a review of trace elements and isotopic composition. *Acta Vulcanol.* 7, 155–166.
- Embey-Isztin, A., Downes, H., James, D.E., Upton, B.G.J., Dobosi, G., Ingram, G.A., Harmon, R.S., Scharbert, H.G., 1993. The petrogenesis of Pliocene alkaline volcanic rocks from the Pannonian basin, Eastern Central Europe. *J. Petrol.* 34, 317–343.
- Esperança, S., Crisci, M., de Rosa, R., Mazzuoli, R., 1992. The role of the crust in the magmatic evolution of the island Lipari (Aeolian Islands, Italy). *Contrib. Mineral. Petrol.* 112, 450–462.
- Frisch, W., Dunkl, I., Kuhlemann, J., 2000. Post-collisional orogeny parallel large scale extension in the Eastern Alps. *Tectonophysics* 327, 239–265.
- Gill, J.B., 1981. *Orogenic Andesites and Plate Tectonics* Springer, New York. 370 pp.
- Gîrbacea, R.A., 1997. The Pliocene to recent tectonic evolution of the Eastern Carpathians (Romania). *Tub. Geowiss. Arb., A Geol. Paläontol. Stratigr.* 35 (136 pp.).
- Gîrbacea, R.A., Frisch, W., 1998. Slab in the wrong place: lower lithospheric mantle delamination in the last stage of the Eastern Carpathians subduction retreat. *Geology* 26, 611–614.
- Green, T.H., Ringwood, A.E., 1968. Genesis of the calc-alkaline igneous rock suites. *Contrib. Mineral. Petrol.* 18, 105–162.
- Harangi, Sz., 2001. Neogene to Quaternary volcanism of the Carpatho–Pannonian region—a review. *Acta Geol. Hung.* 44, 223–258.
- Harangi, Sz., Vaselli, O., Tonarini, S., Szabó, Cs., Harangi, R., Coradossi, N., 1995. Petrogenesis of Neogene extension-related alkaline volcanic rocks of the little Hungarian plain volcanic field (Western Hungary). *Acta Vulcanol.* 7, 173–187.
- Harangi, Sz., Downes, H., Kósa, L., Szabó, Cs., Thirlwall, M.F., Mason, P.R.D., Matthey, D., 2001. Almandine garnet in calc-alkaline volcanic rocks of the Northern Pannonian basin (Eastern-Central Europe): geochemistry, petrogenesis and geodynamic interpretations. *J. Petrol.* 42, 1813–1843.
- Hawkesworth, C.J., O’Nions, R.K., Pankhurst, P.J., Hamilton, P.J., Evensen, N.M., 1977. A geochemical study of island-arc and back-arc tholeiites from the Scotia Sea. *Earth Planet. Sci. Lett.* 36, 253–262.
- Horváth, F., 1993. Towards a mechanical model for the formation of the Pannonian Basin. *Tectonophysics* 226, 333–357.
- Huismans, R.S., Podladchikov, Y.I., Cloetingh, S., 2001. Dynamic modelling of the transition from passive to active rifting, application to the Pannonian basin. *Tectonics* 20, 1021–1039.
- James, D.E., 1981. The combined use of oxygen and radiogenic isotopes as indicators of crustal contamination. *Annu. Rev. Earth Planet. Sci.* 9, 311–344.
- James, D.E., Murcia, L.A., 1984. Crustal contamination in northern Andean volcanics. *J. Geol. Soc. (Lond.)* 141, 823–830.
- Kapezhinskis, P., McDermott, F., Defant, M.J., Hochstaedter, A., Drummond, M.S., Hawkesworth, C.J., Koloskov, A., Maury, R.C., Bellon, H., 1997. Trace element and Sr–Nd isotopic constraints on a three-component model of Kamchatka Arc petrogenesis. *Geochim. Cosmochim. Acta* 61, 577–600.
- Konečny, V., Lexa, J., Hojstrčová, V., 1995. The central Slovakia Neogene volcanic field: a review. *Acta Vulcanol.* 7, 63–79.
- Kováč, M., Nogymarossy, A., Oszczypko, N., Ślączka, A., Csontos, L., Mărănteanu, M., Maťenco, L., Márton, M., 1998. Palinspastic reconstruction of the Carpathian Pannonian region during the Miocene. In: Rakus, M. (Ed.), *Geologic Development of the Western Carpathians*. GSSR, Bratislava, pp. 189–217.
- Kovacs, M., 2002. Petrogenesea rocilor magmatische de subducție din aria central-sud-estică a Munților Gutâi Cluj-Napoca, Dacia. In Romanian, 201 pp.
- Lexa, J., Konečny, V., 1998. Geodynamic aspects of the Neogene to Quaternary volcanism. In: Rakus, M. (Ed.), *Geologic Development of the Western Carpathians*. GSSR, Bratislava, pp. 219–240.

- Lexa, J., Konečny, V., Kováč, M., Nemčok, M., 1995. Relationship among convergence, back-arc extension and volcanism in the Western Carpathians during Neogene. Stara Lesna Europrobe-Pancardi Workshop, Abstract. Geological Institute, Slovak Academy of Sciences, p. 65.
- Márton, E., 1987. Paleomagnetism and tectonics in the Mediterranean region. *J. Geodyn.* 7, 33–57.
- Márton, E., 2000. The Tisza megatectonic unit in the light of paleomagnetic data. *Acta Geol. Hung.* 43, 329–343.
- Márton, E., Márton, P., 1996. Large scale rotations in North Hungary during the Neogene as indicated by paleomagnetic data. In: Morris, A., Tarling, D.H. (Eds.), Paleomagnetism and Tectonics of the Mediterranean Region. Spec. Publ.-Geol. Soc. Lond., vol. 105, pp. 153–173.
- Márton, E., Pécsay, Z., 1998. Correlation and dating of the Miocene ignimbritic volcanics in the Bükk foreland, Hungary: complex evaluation of paleomagnetic and K/Ar isotope data. *Acta Geol. Hung.* 41, 467–476.
- Márton, E., Vass, D., Tunyi, I., 2000. Counterclockwise rotations of the Neogene rocks in the East Slovak basin. *Geol. Carpath.* 51, 159–168.
- Mason, P., Downes, H., Seghedi, I., Szakács, A., Thirlwall, M.F., 1995. Low-pressure evolution of magmas from the Călimani, Gurghiu and Harghita mountains. *Acta Vulcanol.* 7, 43–53.
- Mason, P., Downes, H., Thirlwall, M.F., Seghedi, I., Szakács, A., Lowry, D., Mattey, D., 1996. Crustal assimilation as a major petrogenetic process in the east Carpathian Neogene and Quaternary continental margin arc, Romania. *J. Petrol.* 37, 927–959.
- Mason, P.R.D., Seghedi, I., Szakács, A., Downes, H., 1998. Magmatic constraints on geodynamic models of subduction in the Eastern Carpathians, Romania. *Tectonophysics* 297, 157–176.
- Maťenco, L., 1997. Tectonic evolution of the outer Romanian Carpathians: constraints from kinematic analysis and flexural modelling. PhD thesis. Vrije Universiteit, Amsterdam. 160 pp.
- Maťenco, L., Bertotti, G., 2000. Tertiary tectonic evolution of the external east Carpathians (Romania). *Tectonophysics* 316, 255–286.
- Meulenkamp, J.E., Kováč, M., Chica, I., 1996. On late Oligocene depocentre migration and the evolution of the Carpathian–Pannonian system. *Tectonophysics* 266, 301–317.
- Nemčok, M., Pospisil, L., Lexa, J., Donelik, R.A., 1998. Tertiary subduction and slab breakoff model of the Carpathian Pannonian region. *Tectonophysics* 295, 307–340.
- Oszczypko, N., 1998. The Western Carpathian foredeep-development of the foreland basin in front of the accretionary wedge and its burial history (Poland). *Geol. Carpath.* 50, 415–431.
- Panaiotu, C., 1998. Paleomagnetic constraints on the geodynamic history of Romania. Reports on Geodesy, vol. 7. Warsaw University of Technology, Warsaw, pp. 205–216.
- Panaiotu, C., 1999. Paleomagnetic studies in Romania. Tectonophysics implications. PhD thesis. University of Bucharest. In Romanian, 265 pp.
- Pătrașcu, S., Panaiotu, C., Şeclăman, M., Panaiotu, C.E., 1994. Timing and rotational motions of Apuseni Mountains, Romania: palaeomagnetic data from Tertiary magmatic rocks. *Tectonophysics* 233, 163–176.
- Pearce, J.A., 1982. Trace element characteristics of lavas from destructive plate boundaries. In: Thorpe, R.S. (Ed.), *Andesite*. Wiley, New York, pp. 525–548.
- Pearce, J.A., Parkinson, I.J., 1993. Trace element models for mantle melting: application to volcanic arc petrogenesis. In: Prichard, H.M., Alabaster, T., Harris, N.B.W., Neary, C.R. (Eds.), *Magmatic Processes and Plate Tectonics*. Spec. Publ.-Geol. Soc., vol. 76, pp. 373–403.
- Peate, D.W., Pearce, J., Hawkesworth, C.J., Colley, H., Edwards, C.M.H., Hirose, K., 1997. Geochemical variation in Vanuatu arc lavas: the role of subducted material and a variable mantle wedge composition. *J. Petrol.* 38, 1331–1358.
- Pécsay, Z., Lexa, J., Szakács, A., Balogh, Kad., Seghedi, I., Konečny, V., Kovacs, M., Márton, E., Székely-Fux, V., Póka, T., Gyarmaty, P., Edelstein, O., Roșu, E., Žec, B., 1995a. Space and time distribution of Neogene–Quaternary volcanism in the Carpatho-Pannonian region. *Acta Vulcanol.* 7, 15–29.
- Pécsay, Z., Edelstein, O., Seghedi, I., Szakács, A., Kovacs, M., Crihan, M., Bernad, A., 1995b. K–Ar datings of the Neogene–Quaternary calc-alkaline volcanic rocks in Romania. *Acta Vulcanol.* 7, 53–63.
- Pécsay, Z., Seghedi, I., Downes, H., Prychodko, M., Mackiv, B., 2000. Geochronological and volcanological study of calc-alkaline volcanic rocks from Transcarpathia, SW Ukraine. *Geol. Carpath.* 51 (2), 83–89.
- Petford, N., Atherton, M.P., 1995. Cretaceous–Tertiary volcanism and syn-subduction crustal extension in northern central Peru. In: Smellie, J.L. (Ed.), *Volcanism Associated to Extension at Consuming Plate Margins*. Spec. Publ.-Geol. Soc., vol. 81, pp. 233–248.
- Póka, T., Zelenka, T., Szakács, A., Seghedi, I., Nagy, G., Simonits, A., 1998. Petrology and geochemistry of the Miocene acidic explosive volcanism of the Bükk foreland, Pannonian basin, Hungary. *Acta Geol. Hung.* 41/4, 437–467.
- Ratschbacher, L., Frisch, W., Linzer, H.-G., Merle, O., 1991. Lateral extrusion in the Eastern Alps: Part 2. Structural analysis. *Tectonics* 10, 257–261.
- Roca, E., Bessereau, G., Jawor, E., Kotarba, M., Roure, F., 1995. Pre-Neogene evolution of the western Carpathians: constraints from the Bohemia–Tatra mountains section (polish western Carpathians). *Tectonics* 14, 855–873.
- Rosenbaum, J.M., Wilson, M., Downes, H., 1997. Multiple enrichment of the Carpathian–Pannonian mantle: Pb–Sr–Nd isotope and trace element constraints. *J. Geophys. Res.* 102 (B7), 14947–14961.
- Roșu, E., Pécsay, Z., Stefan, A., Popescu, G., Panaiotu, C., Panaiotu, C.E., 1997. The evolution of the Neogene volcanism in the Apuseni mountains (Romania): constraints from new K/Ar data. *Geol. Carpath.* 48 (6), 353–359.
- Roșu, E., Szakács, A., Downes, H., Seghedi, I., Pécsay, Z., Panaiotu, C., 2001. The origin of Neogene calc-alkaline and alkaline magmas in the Apuseni Mountains, Romania: the adakite connection. *Rom. J. Miner. Depos.* 71 (Suppl. 2), 3–23 (ABCD-Geode 2001 workshop).
- Roure, F., Roca, E., Sassi, W., 1993. The Neogene evolution of the outer Carpathians Flysch units (Poland, Ukraine and Romania): kinematics of foreland fold-and-thrust belt system. *Sediment. Geol.* 86, 177–201.

- Royden, L.H., 1988. Late cenozoic tectonics of the Pannonian basin system. In: Royden, L., Horvath, F. (Eds.), *The Pannonian Basin: A Study in Basin Evolution*. AAPG Memoir, vol. 45, pp. 27–48.
- Royden, L.H., 1993. The tectonic expression slab pull at continental convergence boundaries. *Tectonics* 12, 303–325.
- Royden, L.H., Burchfiel, B.C., 1989. Are systematic variations in thrust-belt style related to plate boundary processes? *Tectonics* 8, 51–61.
- Royden, L.H., Horvath, F., Burchfiel, B.C., 1982. Transform faulting, extension and subduction in the Carpatho-Pannonian region. *Bull. Geol. Soc. Am.* 93, 717–725.
- Salters, V.J.M., Hart, S.R., Pantó, Gy., 1988. Origin of late cenozoic volcanic rocks of the Carpathian arc, Hungary. In: Royden, L., Horvath, F. (Eds.), *The Pannonian Basin: A study in Basin evolution*. AAPG Memoir, vol. 45, pp. 279–292.
- Săndulescu, M., 1984. *Geotectonica României Tehnica*, Bucharest. In Romanian, 366 pp.
- Săndulescu, M., 1988. Cenozoic tectonic history of the Carpathians. In: Royden, L., Horvath, F. (Eds.), *The Pannonian Basin: A Study in Basin Evolution*. AAPG Memoir, vol. 45, pp. 17–25.
- Seghedi, I., Szakács, A., Udrescu, C., Stoian, M., Grabari, G., 1987. Trace element geochemistry of the south Harghita volcanoes (East Carpathians). Calc-alkaline and shoshonitic association. *D. S. Inst. Geol. Geofiz.* 72–73/1, 381–397.
- Seghedi, I., Szakács, A., Mason, P.R.D., 1995. Petrogenesis and magmatic evolution in the east Carpathians Neogene volcanic arc (Romania). *Acta Vulcanol.* 7, 135–145.
- Seghedi, I., Balintoni, I., Szakács, A., 1998. Interplay of tectonics and Neogene post-collisional magmatism in the intracarpathian area. *Lithos* 45, 483–499.
- Seghedi, I., Downes, H., Pécsay, Z., Thirlwall, M.F., Szakács, A., Prychodko, M., Matthey, D., 2001. Magmagenesis in a subduction-related post-collisional volcanic arc segment: the Ukrainian Carpathians. *Lithos* 57, 237–262.
- Sekine, T., Willey, P.J., 1982. The system granite–peridotite–H₂O at 30 kbar, with application to hybridization in subduction zone magmatism. *Contrib. Mineral. Petrol.* 81, 190–202.
- Singer, B.S., Leeman, W.P., Thirlwall, M.F., Roger, N.W.E., 1996. Does fracture zone subduction increase sediment flux and mantle melting in subduction zones? Trace element evidence from Aleutian arc basalt. In: Bebout, G.E., Scholl, D.W., Kirby, S.H., Platt, J.P. (Eds.), *Subduction Top to Bottom*. Geophysical Monograph, vol. 96, pp. 285–291.
- Smith, T.E., Thirlwall, M.F., MacPherson, C., 1996. Trace element and isotope geochemistry of the volcanic rocks of Bequia, Grenadine island, Lesser Antilles arc: a study of subduction enrichment and intra-crustal contamination. *J. Petrol.* 37, 117–148.
- Sperner, B., Lillie, R.J., 2001. Vertical motions related to ocean subduction and continental collision: example from the Eastern Carpathians (Abstract). E.U.G., XI Journal of the Conference Abstracts, vol. 6 (1), p. 1433.
- Sun, S., McDonough, W.F., 1989. Chemical and isotopic systematics of oceanic basalts: implications for mantle compositions and processes. In: Saunders, A.D., Norry, M.J. (Eds.), *Magma in the Ocean Basins*. Spec. Publ.-Geol. Soc., vol. 42, pp. 313–345.
- Szabó, Cs., Harangi, Sz., Csontos, L., 1992. Review of Neogene and Quaternary volcanism of the Carpathian–Pannonian region. *Tectonophysics* 208, 243–256.
- Szakács, A., 2000. Petrologic and tephrologic study of Lower Badian volcanic tufts from NW of Transylvanian Basin. PhD thesis. University of Bucharest. In Romanian, 168 pp.
- Szakács, A., Seghedi, I., Pécsay, Z., 1993. Peculiarities of south Harghita Mts. as terminal segment of the Carpathian Neogene to Quaternary volcanic chain. *Rev. Roum. Geol.* 37, 21–36.
- Szakács, A., Downes, H., Roșu, E., Seghedi, I., Pécsay, Z., 1999. Relationships between geochemical features and age of Neogene volcanic rocks in the Apuseni Mts., Romania. *Rom. J. Tecton. Reg. Geol.* 77 (Suppl. 1), 36.
- Tatsumi, Y., Eggins, S., 1995. Subduction Zone Magmatism. Blackwell, Cambridge, MA. 211 pp.
- Thirlwall, M.F., Smith, T.E., Graham, A.M., Theodorou, N., Hollings, J.P., Davidson, J.P., Arculus, R.J., 1994. High field strength element anomalies in arc lavas: source or process? *J. Petrol.* 35, 819–838.
- Thirlwall, M.F., Graham, A.M., Arculus, R.J., Harmon, R.S., Macpherson, C.G., 1996. Resolution of the effects of crustal assimilation, sediment subduction and fluid transport in island arc magmas: Pb–Sr–Nd–O isotope geochemistry of Grenada, Lesser Antilles. *Geochim. Cosmochim. Acta* 23, 4785–4810.
- Vaselli, O., Downes, H., Thirlwall, M., Dobosi, G., Coradossi, N., Seghedi, I., Szakács, A., 1995. Ultramafic xenoliths in Plio-Pleistocene alkali basalts from the Eastern Transylvanian basin: depleted mantle enriched by vein metasomatism. *J. Petrol.* 36, 23–53.
- Vass, D., 1995. The origin and disappearance of Hungarian Paleogene basin and short-term lower Miocene basins in Northern Hungary and southern Slovakia. *Slovak Geol. Mag.* 1–1, 81–95.
- Vroon, P.Z., van Bergen, M.J., White, W.M., Varekamp, J.C., 1993. Sr–Nd–Pb isotope systematics of the Banda arc, Indonesia: combined subduction and assimilation of continental material. *J. Geophys. Res.* 98 (B12), 22349–22366.
- Wortel, M.J.R., Spakman, W., 2000. Subduction and slab detachment in the Mediterranean–Carpathian region. *Science* 290, 1910–1917.
- Xu, J.-F., Shinjo, R., Defant, M.J., Wang, Q., Rapp, R.P., 2002. Origin of Mesozoic adakitic intrusive rocks in the Ningzhen area of East China: partial melting of delaminated lower continental crust? *Geology* 30, 1111–1114.
- Yagodzinski, G.M., Lees, M.L., Churikova, T.G., Dorendorf, F., Wöerner, G., Volynets, O.N., 2001. Geochemical evidence for the melting of subducting oceanic lithosphere at plate edges. *Nature* 409, 500–504.
- Zweigel, P., 1997. The Tertiary tectonic evolution of the eastern Carpathians (Romania): orogenic arc formation in response to microplate movements. *Tüb. Geowiss. Arb.* 33 (127 pp.).